Journal of Neuroinflammation

RESEARCH

Open Access

Taprenepag restores maternal–fetal interface homeostasis for the treatment of neurodevelopmental disorders

Kai Wang[1,2†], Shufen Zhang[1†], Yunxia Wang[1], Xiaomei Wu[1], Lijuan Wen[3], Tingting Meng[1,2], Xiangyu Jin[3], Sufen Li[1], Yiling Hong[1], Jia Ke[1], Yichong Xu[1], Hong Yuan[1,2] and Fuqiang Hu[1,2,4*]

Abstract

Background and purpose Neurodevelopmental disorders (NDDs) are characterized by abnormalities in brain development and neurobehaviors, including autism. The maternal–fetal interface (MFI) is a highly specialized tissue through which maternal factors affect fetal brain development. However, limited research exists on restoring and maintaining MFI homeostasis and its potential impact on NDDs. This study explores the role of placental indoleamine 2,3-dioxygenase (IDO-1) in MFI homeostasis and fetal brain development.

Experimental Approach The maternal-fetal barrier was disrupted by sodium valproate (VPA) in pregnant mice, whose offspring show typical autism-like behaviors. Ultrastructural analysis and flow cytometric analysis were conducted to observe the morphological and immune system changes. Behavioral tests and immunofluorescence staining was used to investigate the ability and mechanism of taprenepag to alleviate the abnormal behaviors of VPA-exposed offspring and normalize the development of serotonergic neurons.

Key results In VPA-exposed pregnant mice, the downregulation of IDO-1 led to maternal immune overactivation and disruption of maternal-fetal barrier, resulting in excessive 5-HT synthesis in the placenta. This process disrupted the development of the serotonergic neuronal system in the offspring, resulting in impaired development of serotonergic neurons, thalamocortical axons, and NDDs in the progeny. However, a single injection of taprenepag at E13.5 ultimately upregulated placental IDO-1 through amplifying the positive feedback loop COX-2/PGE_2/PTGER-2/IDO-1 and abolished these alterations.

Conclusion Taprenepag improved autism-like behaviors in the offspring of VPA-exposed mice by addressing placental IDO-1 downregulation. This study highlights the potential of targeting IDO-1 to mitigate MFI disruption and NDD development.

Keywords Placental tryptophan metabolism, Neurodevelopmental disorders, Maternal-fetal barrier, Immune disorder, IDO-1

†Kai Wang and Shufen Zhang contributed equally to this work.

*Correspondence:
Fuqiang Hu
hufq@zju.edu.cn
[1]College of Pharmaceutical Sciences, Zhejiang University, 866 Yuhangtang Road, Hangzhou 310058, PR China
[2]Jinhua Institute of Zhejiang University, Jinhua 321299, PR China
[3]Department of Pharmacy, The Cancer Hospital of the University of Chinese Academy of Sciences (Zhejiang Cancer Hospital), Institute of Basic Medicine and Cancer (IBMC), Chinese Academy of Sciences, Hangzhou, Zhejiang 310022, PR China
[4]National Engineering Research Center for Modernization of Traditional Chinese Medicine-Hakka Medical Resources Branch, College of Pharmacy, Gannan Medical University, Ganzhou 341000, PR China

Introduction

Neurodevelopmental disorders (NDDs) are abnormalities in brain development and characterized by cognitive impairment and neurobehavioral abnormalities [1]. Autism spectrum disorders (ASD) are a common type of NDDs characterized by social deficits, repetitive stereotyped behavior, and lack of interest [2]. In 2018, ASD affected nearly 1 in 36 children in the United States, according to the Centers for Disease Control and Prevention (CDC) [3]. The triggers of autism remain elusive, but genetic, developmental and environmental factors clearly play important roles [4]. Maternal events during pregnancy have been a key focus of research, with high-risk exposure factors such as a high-fat diet, valproate exposure, and gestational diabetes mellitus reportedly linked to the occurrence of autism in offspring [5, 6].

Among ASD caused by various environmental factors, a common maternal complication is the imbalance of homeostasis at the maternal-fetal interface (MFI), often leading to immune disorders in the placenta and disruption of the maternal-fetal barrier function. The MFI is composed of the maternally derived decidua and the fetally derived placenta [7]. The MFI is primarily an immunological term, encompasses not only the immunosuppressive microenvironment established through interactions between maternal and fetal cells but also the barrier function provided by placental trophoblast cells. The decidua houses three main types of immune cells: decidual natural killer cells (dNK), decidual macrophages (dM) and T cells. Immune disorders in the placenta have been associated with adverse fetal outcomes, such as increased miscarriages due to reduced expansion of natural regulatory T cells [8], maternal immune activation caused by hyperproliferation of effector T lymphocytes [9], decidualization deficiency resulting from decidual natural killer cell dysfunction [10], and embryo implantation arrest due to depletion of decidual macrophages [11].

The placenta plays a crucial role in regulating the bidirectional exchange of substances, maintaining maternal tolerance, and minimizing fetal exposure to harmful agents [12]. The placental barrier serves as a critical interface between maternal and fetal circulation, consisting of the apical (brush border, maternal facing) and basal (fetal facing) plasma membranes of syncytiotrophoblast cells, along with fetal endothelial cells [13]. Notably, a single layer of continuous multinucleated syncytiotrophoblast cells, which lines the outermost surface of the placental villus tree, is primarily responsible for this barrier function [7]. Furthermore, the placental barrier acts as a component of the innate immune system, thus expanding the concept of the MFI. The maternal-fetal barrier (MFB) encompasses a broader definition of the barrier function between the mother and fetus, integrating both the placental and amniotic barriers. The innermost epithelial layer of the amnion functions as an immune barrier that protects the fetus [14].

Recent studies in neuroplacentology have been examining the impact of the placenta on fetal neurodevelopment through the production of hormones and neurotransmitters, influencing immediate and long-lasting neurodevelopment through the placenta-brain axis [15, 16]. Placental dysfunction and disruption of barrier function are believed to be significant contributors to NDDs, including placental ischemia in conditions like preeclampsia [17] and disruption of MFB induced by zika virus infection [18]. Additionally, substantial evidence suggests that placental developmental disorders are closely linked to the occurrence of autism, such as mitochondrial dysfunction [19], changes in transplacental barrier permeability [20], and increased leakage of trophoblast inclusions [21].

The above evidence highlights the correlation between NDDs and placental immune dysfunction, as well as the disruption of the MFB. However, there is a research gap concerning the interplay between these factors and their effects on fetal neurodevelopment. It prompts the question of whether improving the function of one aspect of the placenta could lead to the recovery of another function, ultimately benefiting the offspring's neurodevelopment. Given the limited research on the MFB, there is a lack of identified regulatory targets. Our focus is on exploring the regulation and preservation of the placental immunosuppressive microenvironment to understand its influence on MFB function and the neural development of offspring.

L-tryptophan (Trp) is an essential precursor for many metabolites, undergoing oxidation to the kynurenine pathway by indoleamine 2,3-dioxygenase (IDO-1) and hydroxylation to the serotonin pathway by Trp hydroxylase 1 (TPH-1) in the placenta [22]. Kynurenine (Kyn) is known to play a role in immune tolerance maintenance, while serotonin (5-hydroxytryptamine, 5-HT) is a crucial monoamine neurotransmitter closely associated with ASD [23]. Studies have shown that fetal neurodevelopment is blunt due to the accumulation of placental 5-HT [24]. Its pathogenesis is mainly explained by the upregulation of TPH-1 enzymatic activity induced by maternal inflammation. Imbalances in placental Trp metabolism have been linked to NDDs in both maternal serotonin transporter (SERT) knock-in mice and models of maternal vitamin D insufficiency [25, 26]. Additionally, disruptions in brain Trp metabolism in infants have been implicated in the development of social deficits [27, 28]. The mechanism by which excess serotonin from the placenta reaches the fetal brain remains unclear, as serotonin cannot easily traverse the MFB or the blood-brain barrier (BBB) [29, 30]. This phenomenon may be

associated with compromised placental barrier function in individuals with autism, although concrete evidence is lacking. Additionally, the specific regulatory mechanisms governing placental Trp metabolism and the potential for restoring balance to improve fetal neurodevelopment are areas of uncertainty in current research.

This research primarily investigates a series of adverse outcomes at the MFI associated with alterations in Trp metabolism following VPA exposure during pregnancy, and its influence on the development of the serotonergic neuronal system in fetal mice. The study aims to enhance the expression of placental IDO-1 through the administration of taprenepag, a prostaglandin E_2 receptor (PTGER-2) agonist, during pregnancy. This approach seeks to regulate tryptophan metabolism, improve placental immune function, and repair the integrity of the placental barrier. Furthermore, we evaluate the effects of taprenepag on serotonergic neurons in fetal mice, as well as its protective and therapeutic impacts on autistic behaviors in the offspring.

Materials and methods

Animals and reagents

Pregnant ICR mice aged 7–8 weeks were purchased from Ziyuan Biotechnology Co., Ltd (Hangzhou, China). Female and male mice were mated overnight at a 2:1 ratio. The presence of a vaginal plug confirmed pregnancy, which was recorded as embryonic day 0.5 (E0.5).

Cell line The human placental choriocarcinoma cell line JEG-3 was purchased from the Institute of Basic Medical Sciences, Chinese Academy of Medical Sciences.

Reagents VPA (Sigma-Aldrich, St. Louis, MO); RU486 (Selleck Chemicals, Shanghai, China); taprenepag, butaprost and linrodostat (MedChemExpress, Shanghai, China); and kynurenine (Aladdin, Shanghai, China).

VPA exposure during pregnancy and dosing regimen

Pregnant mice were injected subcutaneously with 600 mg/kg valproic acid saline (VPA) or saline only (control) in the neck region at E12.5[31]. To ensure successful induction of ultrasonic defects, a final dose of 600 mg/kg is recommended [32]. The timing of drug administration is critical; the final chorioallantoic placenta begins to form at E12.5, coinciding with the establishment of the maternal decidua, junctional zone, and labyrinthine zone [7, 33]. Administering VPA at this stage facilitates a more efficient examination of its detrimental effects on the MFB. Furthermore, the model was established at E12.5, with drug treatment conducted at E13.5 to modulate placental function, followed by pharmacodynamic evaluation at E14.5. This timeline underscores the relationship between placental function regulation and fetal mouse neurodevelopment, particularly since the fetal mouse blood-brain barrier has not yet formed by this stage (E15 days) [34]. For specific animal experiment conditions and experimental arrangements, please see the supplementary materials.

The different drug treatment regimens used were as follows.

For studies in Figs. 1A, 2A, 3A and 4, the VPA-exposed pregnant mice were subcutaneously injected with 0.05 mg/kg RU486 (VPA + RU486), 0.5 mg/kg taprenepag (VPA + Tap), 0.5 mg/kg kynurenine (VPA + Kyn) or 0.5 mg/kg butaprost (VPA + But) at E13.5 [35]. Pregnant mice in the VPA and control groups received an equal volume of saline at E13.5. Pregnant mice were euthanized and placentas and fetuses were collected 24 h after drug administration for subsequent experiments.

For the behavioral evaluation of offspring mice in Fig. 5A, VPA-exposed pregnant mice were injected subcutaneously with 0.5 mg/kg Tap (VPA + Low Tap) or 2.5 mg/kg Tap (VPA + High Tap) s.c. at E13.5. Pregnant mice in the other groups were treated as described above. Pregnant mice were housed and used to nurture offspring mice. The day of birth was represented as P0. The offspring mice were caged at P21, and behavioral evaluations were conducted at P45.

For the IDO1 antagonism experiments in Fig. 6A, VPA-exposed pregnant mice were injected subcutaneously with 0.5 mg/kg taprenepag (VPA + Tap), 5 mg/kg linrodostat (VPA + Lin) or 0.5 mg/kg taprenepag and 5 mg/kg linrodostat (VPA + Tap + Lin) at E13.5. Pregnant mice in the VPA and control groups received an equal volume of saline at E13.5. Some pregnant mice were euthanized at E14.5, and the related tissues were collected for subsequent experiments. The other pregnant mice were retained until the offspring were weaned. The offspring were subjected to behavioral analysis and immunohistochemical examination.

Maternal immune activation and dosing regimen

Pregnant mice were injected intraperitoneally with 20 mg/kg polyinosinic: polycytidylic acid [poly (I: C)] (Sigma) to stimulate maternal immune activation (MIA) or saline only (control) at E12.5 [36, 37]. For studies in Fig. 7A, pregnant mice in the poly (I: C) + Tap and control + Tap groups were injected subcutaneously with 0.5 mg/kg taprenepag at E13.5. Pregnant mice in the VPA and control groups received an equal volume of saline at E13.5. Pregnant mice were housed and used to nurture offspring mice until P11.

Placental gadolinium leakage monitored by MRI, ICP-MS, TEM and SEM

At E14.5 (24 h after drug administration), the placenta barrier integrity of pregnant mice in the control, VPA

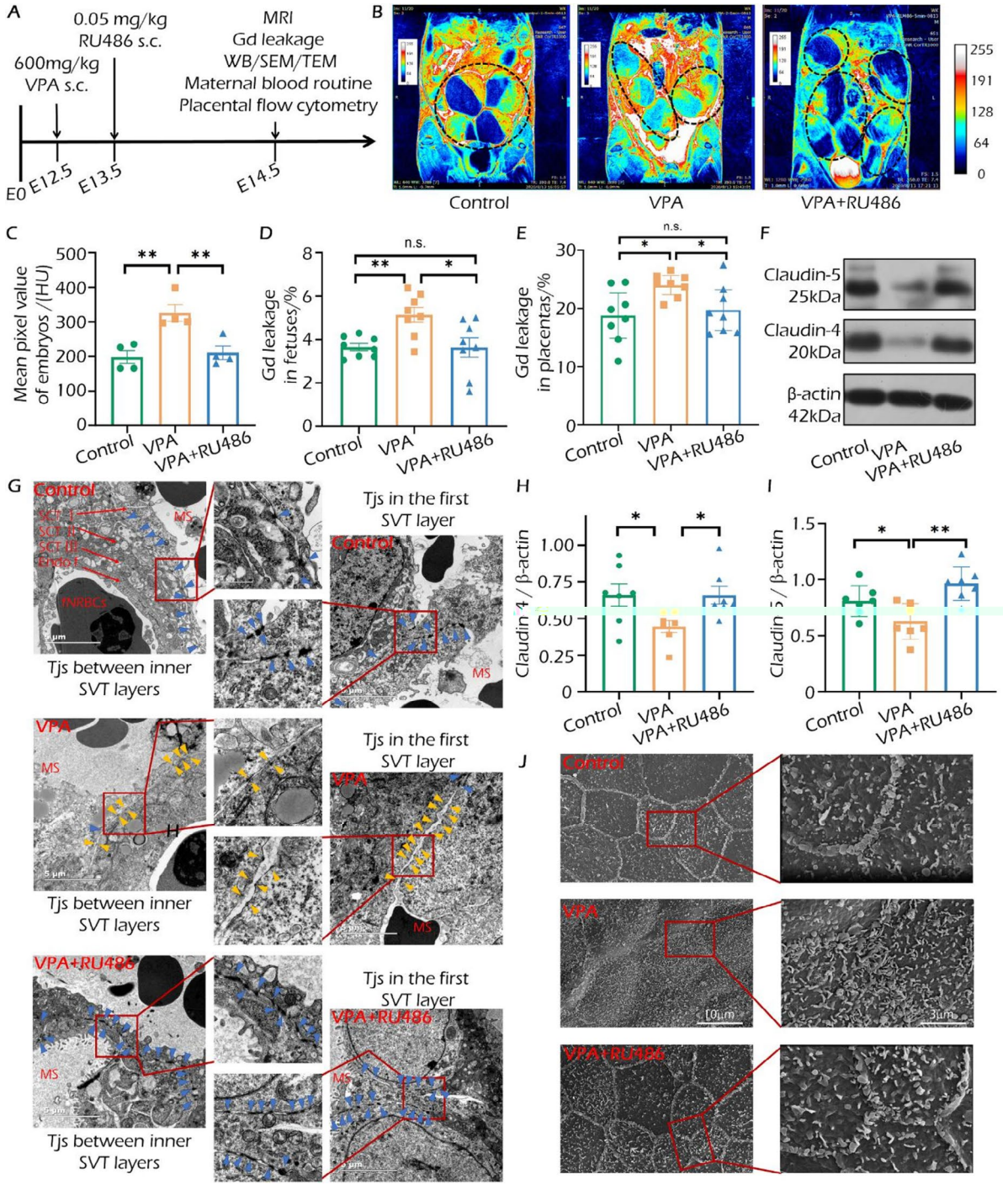

Fig. 1 VPA exposure during pregnancy disrupted the MFB while RU486 treatment alleviated VPA induced damage. (**A**) Experimental flow chart. (**B**) Placental and fetal gadolinium leakage monitored by MRI. The black circle in the picture represents the fetus and placenta. (**C**) The mean pixel value of each fetus in the postcontrast images of A. (Hounsfield units, HU), ($n = 4$, pregnant mice, respectively). (**D**) and (**E**) The Gd leakage into fetuses (**C**) and placentas (**D**) from maternal blood was quantified by ICP-MS. ($n = 8$ dams, respectively). The gadolinium leakage into the placenta or fetus was calculated as the ratio of the Gd concentration of the placenta or fetus and the Gd concentration of maternal blood. (**F**) The expression levels of Tjs (claudin-5 and claudin-4) in placentas at E14.5. (**G**) The ultrastructure of TJs complexes expressed on the amniotic epithelium was visualized by SEM. (**H**) and (**I**) Semi-quantification of the Western blot results of claudin-4 and claudin-5 (**F**) in placentas at E14.5. ($n = 7$ dams, respectively). (**J**) The ultrastructure of TJs in placental syncytiotrophoblast cells (SCTs) was observed by TEM. fNRBCs: fetal nucleated red blood cells. Endo f: fetal endothelial cells. MS: maternal blood sinus. SCT I with microvilli contacts with the MS directly. The yellow triangle indicates loosely bound Tjs or cracks. The blue triangle indicates the normal Tjs. Statistics were calculated by one-way ANOVA with Dunnett's post hoc test for (**C**), (**D**), (**E**), (**H**) and (**I**). The statistical significance is denoted by ns, not significant; $^{*}P < 0.05$; $^{**}P < 0.01$. The graphs show the mean ± SEM

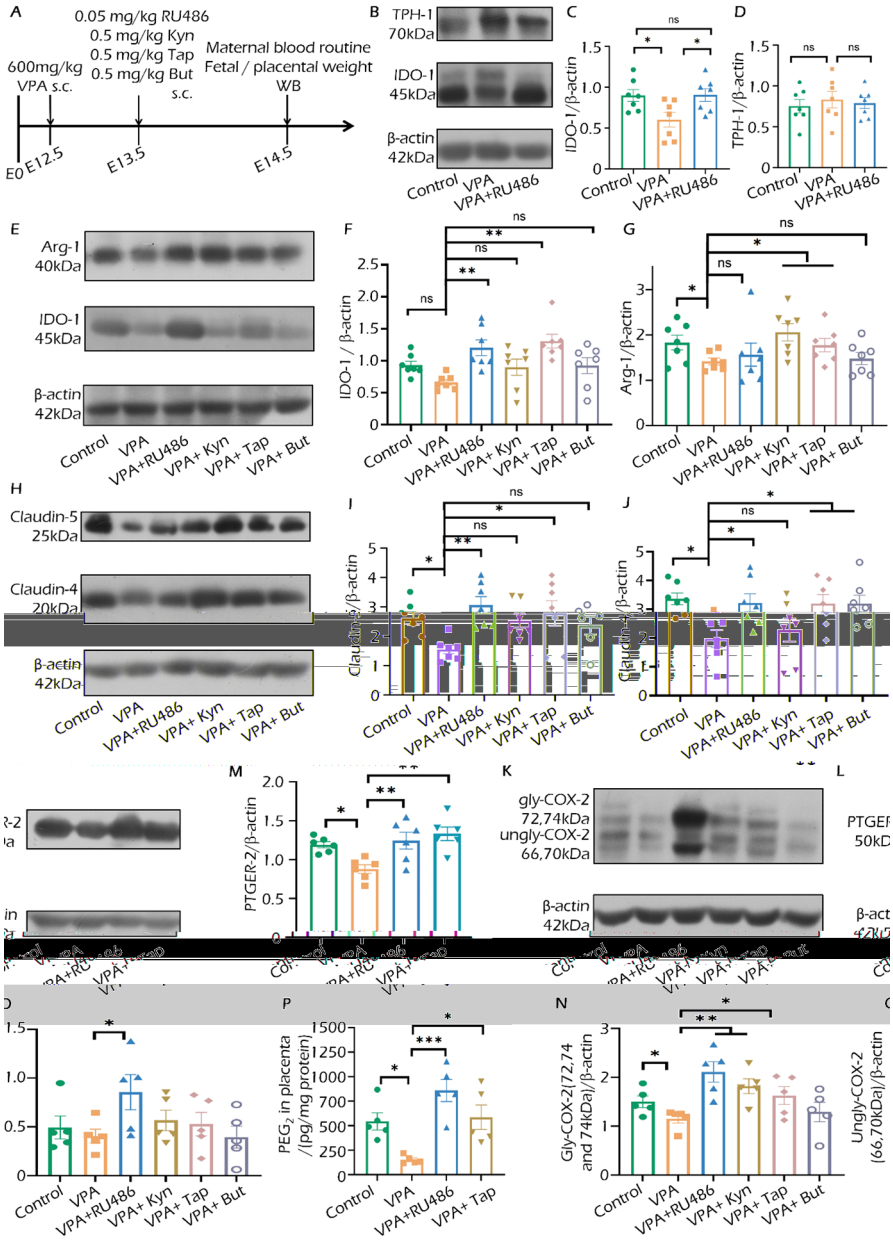

Fig. 2 Taprenepag upregulated placental IDO-1 expression through COX-2/PGE_2/PTGER-2 in pregnant mice exposed to VPA. (**A**) Experimental flow chart. (**B**), (**C**) and (**D**) The expression levels and semiquantification results of the Western blot results of IDO-1 and TPH-1 in the placenta at E14.5. ($n=7$ dams, respectively). (**E**) (**F**) and (**G**) The expression levels and semiquantification results of IDO-1 and Arg-1 (a marker for dM2 cells) after drugs intervention. ($n=7$ dams, respectively). (**H**) (**I**) and (**J**) The expression levels and semiquantification results of Tjs (claudin-5 and claudin-4) in the placenta. ($n=6$ dams in group But of claudin-5. ($n=7$ dams in other group, respectively). (**K**) The expression levels of COX-2 (66 and 70 kDa: the inactive and hypoglycosylated COX-2 precursor; 72 and 74 kDa: active and hyperglycosylated mature COX-2) in the placenta. (**L**) The expression levels of PTGER-2 in the placenta. (**M**) Semiquantification results of the Western blot results of PTGER-2. ($n=6$ dams, respectively). (**N**) and (**O**) Semiquantification results of glycosylated mature Gly-COX-2 and ungly-COX-2 precursor in placenta. ($n=5$ dams, respectively). (**P**) The level of PGE_2 in the placenta was measured by ELISA (pg/mg protein). ($n=5$ dams, respectively). Statistics were calculated by one-way ANOVA with Dunnett's post hoc test for (**C**), (**D**), (**F**), (**F**), (**G**), (**I**), (**J**), (**M**), (**N**), (**O**) and (**P**). The statistical significance is denoted by ns, not significant; $^{*}P<0.05$; $^{**}P<0.01$; $^{***}P<0.001$. The graphs show the mean ± SEM

and VPA+RU486 groups ($n=4$) was evaluated by gadodiamide-contrast enhanced magnetic resonance imaging (MRI, Timemedical, 9T/110). Pre-contrast images were acquired via a T1-weighted two-dimensional spin-echo sequence (2D-SE) as previously described [38]. Each pregnant mouse was injected i.v. with 60 μL of gadodiamide contrast agent (0.05 mM Omniscan, GE Healthcare, Shanghai, China) [39]. Postcontrast images were obtained 20 min after gadodiamide injection. The final image was processed by ImageJ software,

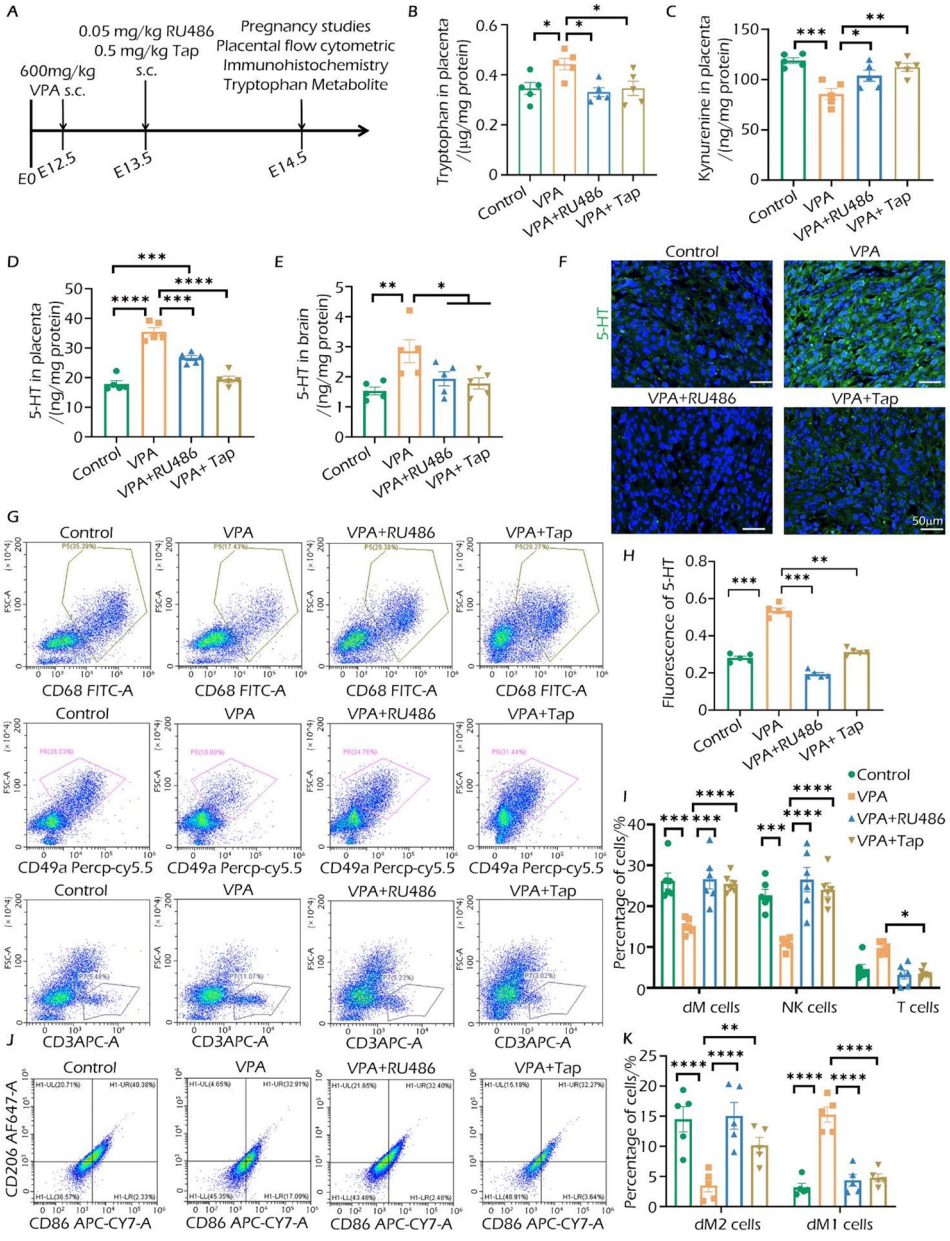

Fig. 3 Taprenepag restored the placental tryptophan metabolism and the abundance of placental immune cells in pregnant mice exposed to VPA. (**A**) Experimental flow chart. (**B**) Placental Trp abundance (μg/mg protein) measured by HPLC at E14.5. ($n = 5$ dams, respectively). (**C**) The placental Kyn abundance (ng/mg protein) measured by the Ehrlich reagents. ($n = 5$ dams, respectively). (**D**) and (**E**) The level of 5-HT in the placenta or fetal brain measured by ELISA. ($n = 5$ dams, respectively). (**F**) Immunofluorescence staining of 5-HT in the placenta. (**G**) Representative figures for flow cytometric clustering of decidua immune cells (T, dM and dNK cells) in placentas. CD68: dM cells. CD49a: dNK cells. CD3: T cells. (**H**) The mean fluorescence intensity of placental 5-HT immunofluorescence staining. ($n = 5$ dams, respectively). (**I**) Flow cytometric clustering of decidua immune cells (T, dM and dNK cells) in the placenta. ($n = 6$ dams, respectively). (**J**) Representative figures for decidual macrophage typing analysis by flow cytometric in placenta. CD206: dM2 cells. CD86: dM1 cells. (**K**) Decidual macrophage typing analysis by flow cytometry in placentas. ($n = 5$ dams, respectively). Statistics were calculated by one-way ANOVA with Dunnett's post hoc test for (**B**), (**C**), (**D**), (**E**) and (**H**) and two-way ANOVA with Tukey's post hoc test for (**I**) and (**K**). Statistical significance is denoted by $^{*}P < 0.05$; $^{**}P < 0.01$; $^{***}P < 0.001$; $^{****}P < 0.0001$. The graphs show the mean ± SEM

with pseudo-colors assigned based on grayscale values to enhance the visibility of image features. The placental barrier integrity of the pregnant mice was calculated as the average pixel value of all fetuses. See supplementary methods.

After MRI, the gadolinium (Gd) content (Gd mass per unit mass of tissues) in the placenta, fetus and maternal blood was determined by inductively coupled-plasma mass spectrometry (ICP-MS, Agilent 7800, Singapore). The leakage of Gd from the placenta or fetus was

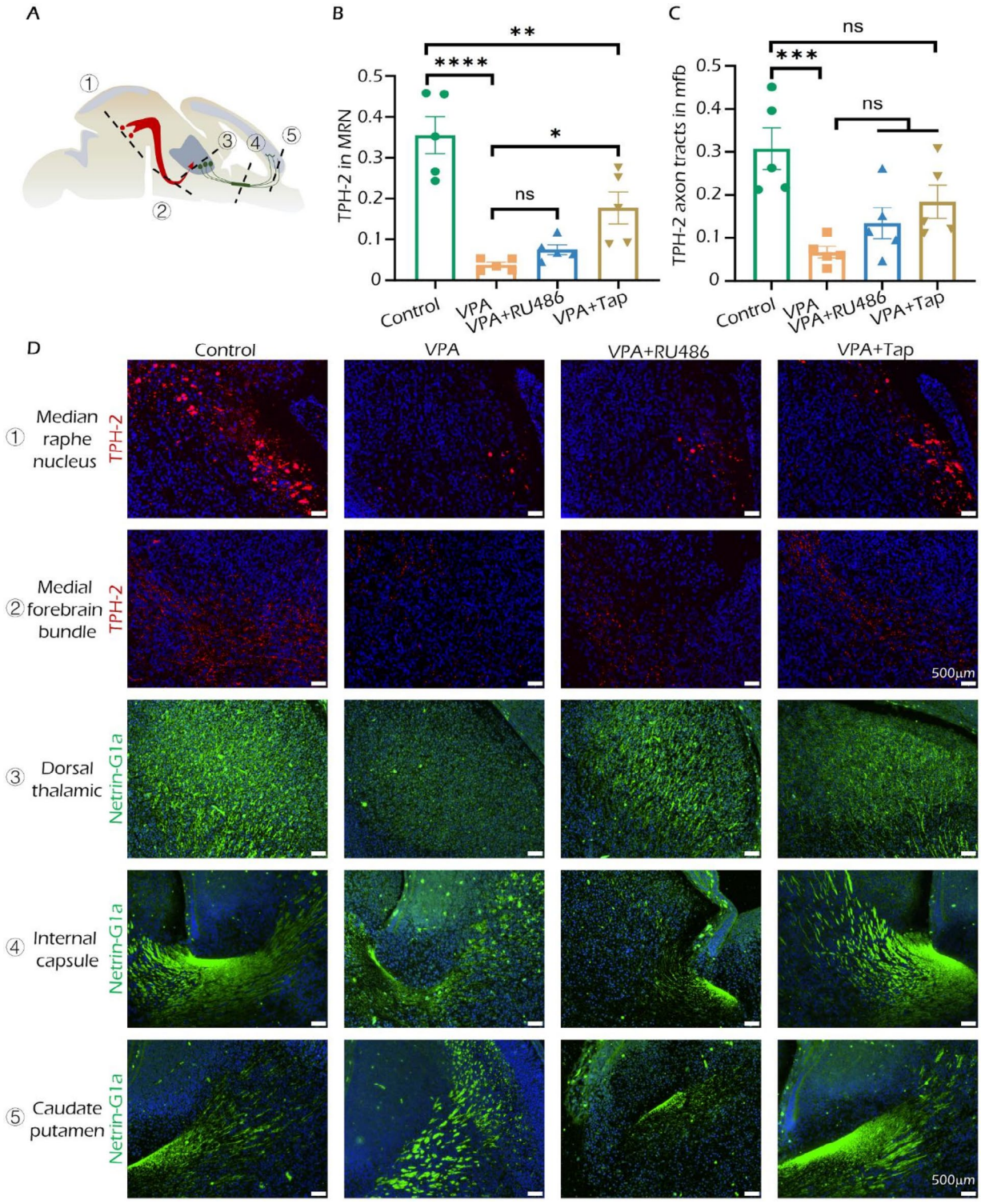

Fig. 4 Taprenepag increased the number of TPH-2$^+$ neurons and improved the development of TCAs in fetuses exposed to VPA. (**A**) Schematic diagram for the neuronal bodies and axons of TPH-2$^+$ neurons and the development of Netrin-G1a$^+$ TCAs and section positions of different slices. VPA-exposed pregnant mice received VPA at E12.5 and drug treatment (0.05 mg/kg RU486 or 0.5 mg/kg taprenepag) at E13.5. The sections were observed 24 h after administration. (**B**) and (**C**) The mean fluorescence intensity of TPH-2$^+$ neuron body immunofluorescence staining in the MRN and TPH-2$^+$ axons in MFB. ($n=5$ dams, respectively). (**D**) Immunofluorescence staining of the neuron bodies and axons of TPH-2$^+$ neurons and Netrin-G1a$^+$ TCAs. Statistics were calculated by one-way ANOVA with Dunnett's post hoc test for (**B**) and (**C**). Statistical significance was denoted by $^*P<0.05$; $^{**}P<0.01$; $^{***}P<0.001$; $^{****}P<0.0001$. The graphs show the mean ± SEM

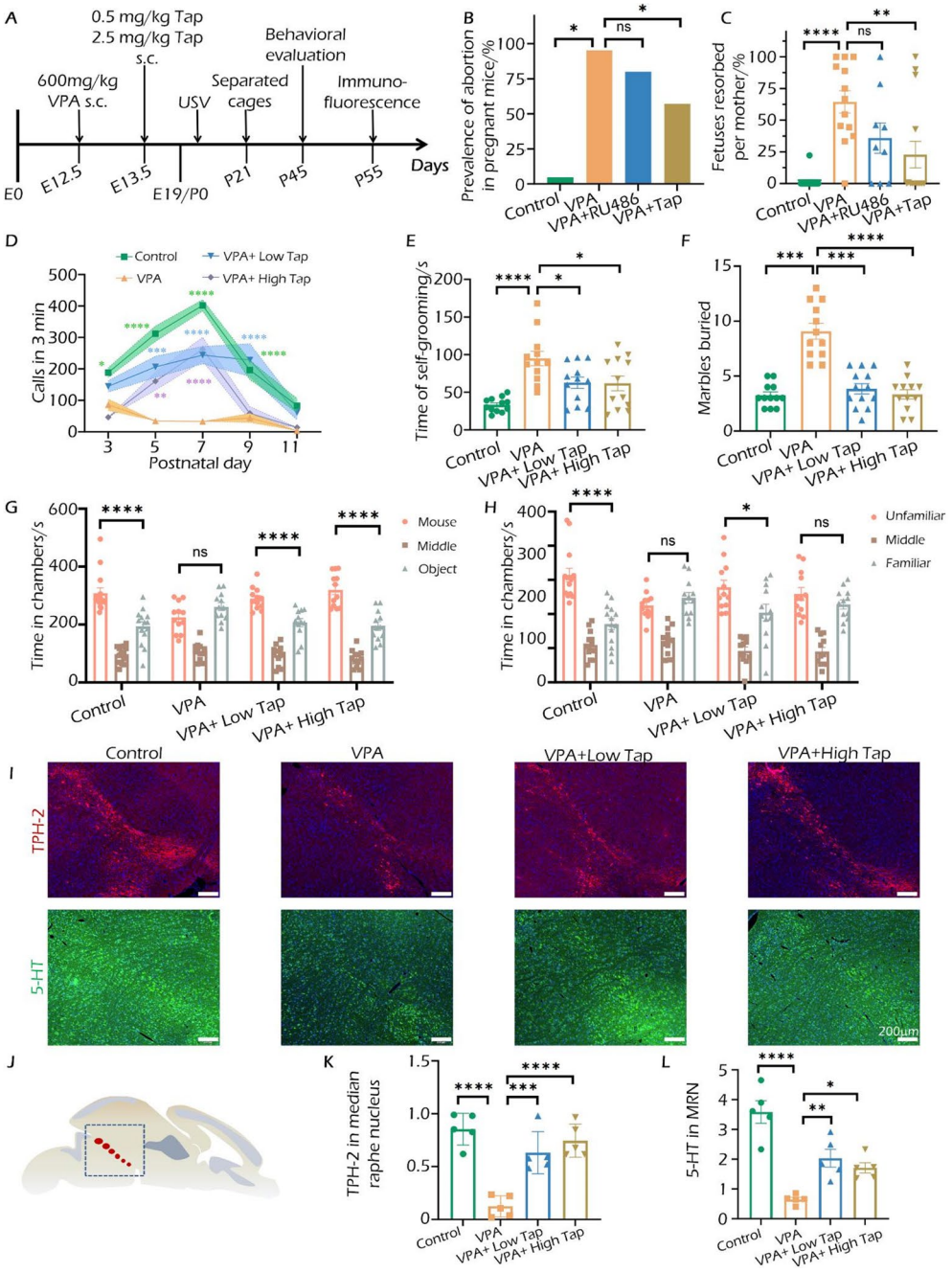

Fig. 5 Taprenepag improved ASD-related behavioral abnormalities and damage to TPH-2$^+$ neurons in offspring exposed to VPA. (**A**) Schematic diagram of the implementation of the experimental plan. VPA-exposed pregnant mice received VPA at E12.5 and Tap treatment (0.5 mg/kg or 2.5 mg/kg) at E13.5. The fetal and placental experiments were carried out at E14.5. USV was conducted at P3-P11, regardless of gender. Behavioral evaluation for male mice began at P45 and was conducted under the following order: (open field, self-grooming behavior, marble burying and three-chamber social interaction assay). (**B**) The percentage of pregnant mice with any (at least one) fetal resorption event (%). (Control and VPA + Tap, $n = 14$ dams; VPA, $n = 13$ dams; VPA + RU486, $n = 9$ dams.) (**C**) The percentage of resorbed fetuses relative to total fetuses. (Control and VPA + Tap, $n = 14$ dams; VPA, $n = 13$ dams; VPA + RU486, $n = 9$ dams.) (**D**) The total calls for pups in 3 min in the isolation-induced distress vocalization assay. ($n = 12$ dams, respectively). (**E**) The cumulative time spent in self-grooming in 10 min. ($n = 12$ dams, respectively). (**F**) The number of marbles buried in 15 min. ($n = 12$ dams, respectively). (**G**) For sociability testing, the time of tested mice spent in the Mouse chamber and Object chamber. ($n = 12$ dams, respectively). (**H**) For the social novelty testing, time of tested mice spent in the Familiar chamber and Unfamiliar chamber. ($n = 12$, respectively). (**I**) Immunofluorescence staining of TPH-2$^+$ neurons and 5-HT in the RN at P55. (**J**) Schematic diagram of TPH-2$^+$ neurons and 5-HT and the positions of sections. (**K**) and (**L**) The mean fluorescence intensity of immunofluorescence staining TPH-2$^+$ and 5-HT in RN. ($n = 5$ dams, respectively). Statistics were calculated by two-tailed $\chi 2$ test for (**B**), one-way ANOVA with Dunnett's post hoc test for (**C**), (**E**), (**F**), (**K**) and (**L**) and two-way ANOVA with Tukey's post hoc test for (**D**), (**G**) and (**H**). Statistical significance was denoted by $^*P < 0.05$; $^{**}P < 0.01$; $^{***}P < 0.001$; $^{****}P < 0.0001$. The graphs show the mean ± SEM

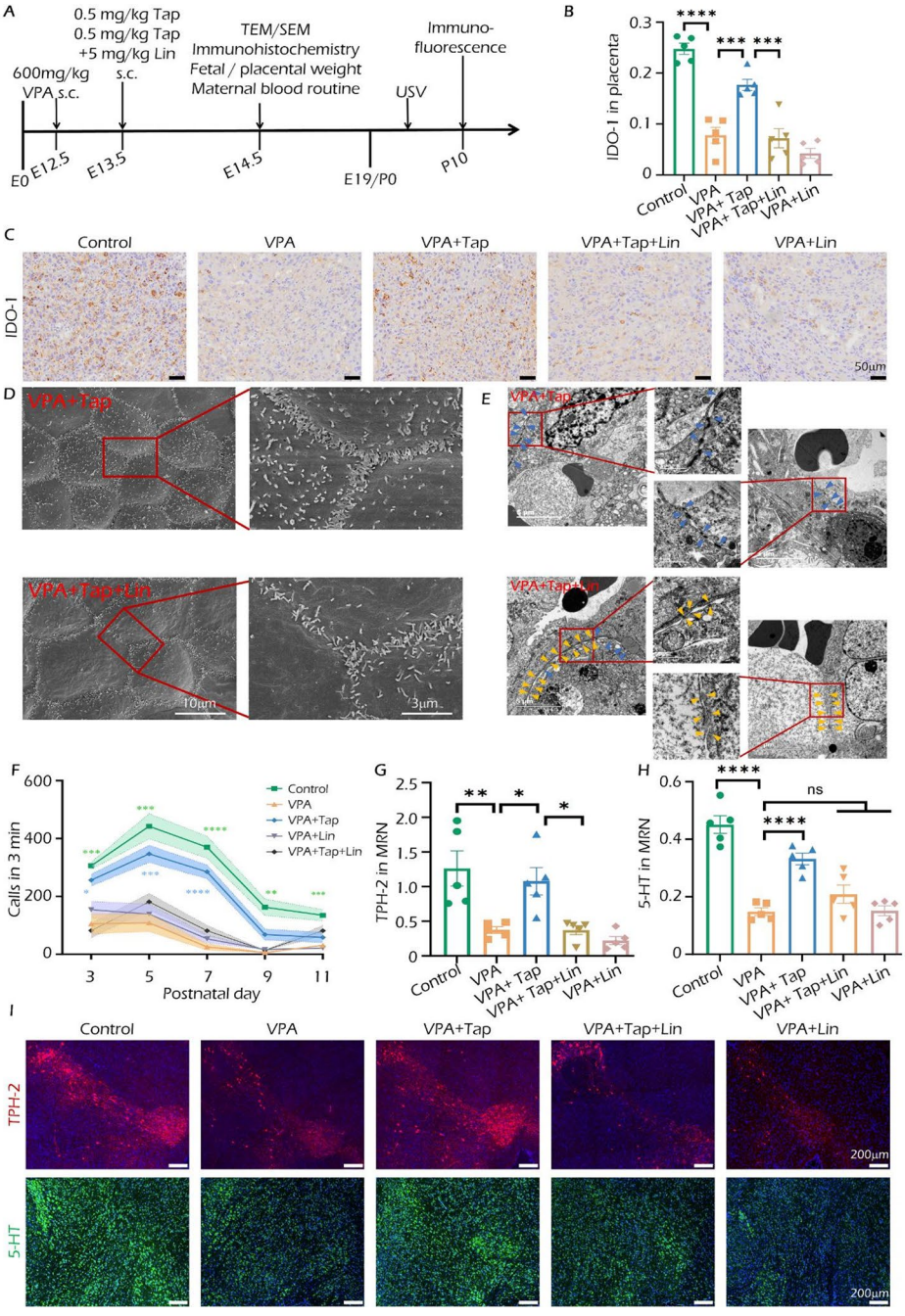

Fig. 6 Inhibition of placental IDO-1 antagonized the therapeutic effect of taprenepag. (**A**) Experimental flow chart. VPA-exposed pregnant mice received VPA at E12.5 and taprenepag treatment (0.5 mg/kg) or taprenepag combined with 5 mg/kg linrodostat at E13.5. USV was conducted on P3-P11, regardless of gender. (**B**) Semiquantitative results of immunohistochemical staining for IDO-1. ($n = 5$ dams, respectively). (**C**) Immunohistochemical staining for placental IDO-1 on E14.5. (**D**) The ultrastructure of tight junction complexes expressed on the amniotic epithelium was visualized by SEM. (**E**) The ultrastructure of tight junctions in placental syncytiotrophoblast cells (SCTs) was observed by TEM. (**F**) The total number of calls for newborn pups in 3 min in the isolation-induced distress vocalization assay. ($n = 12$, "n" represents offspring from different dams). (**G**) and (**H**) The mean fluorescence intensity of immunohistochemical staining for TPH-2$^+$ and 5-HT in the RN of newborn pups. ($n = 5$ dams, respectively). (**I**) Immunofluorescence staining of TPH-2$^+$ neurons and 5-HT in newborn MRN pups at P10. Statistics were calculated by one-way ANOVA with Dunnett's post hoc test for (B), (G) and (H) and two-way ANOVA with Tukey's post hoc test for (**F**). Statistical significance was denoted by $^*P < 0.05$; $^{**}P < 0.01$; $^{***}P < 0.001$; $^{****}P < 0.0001$. The graphs show the mean ± SEM

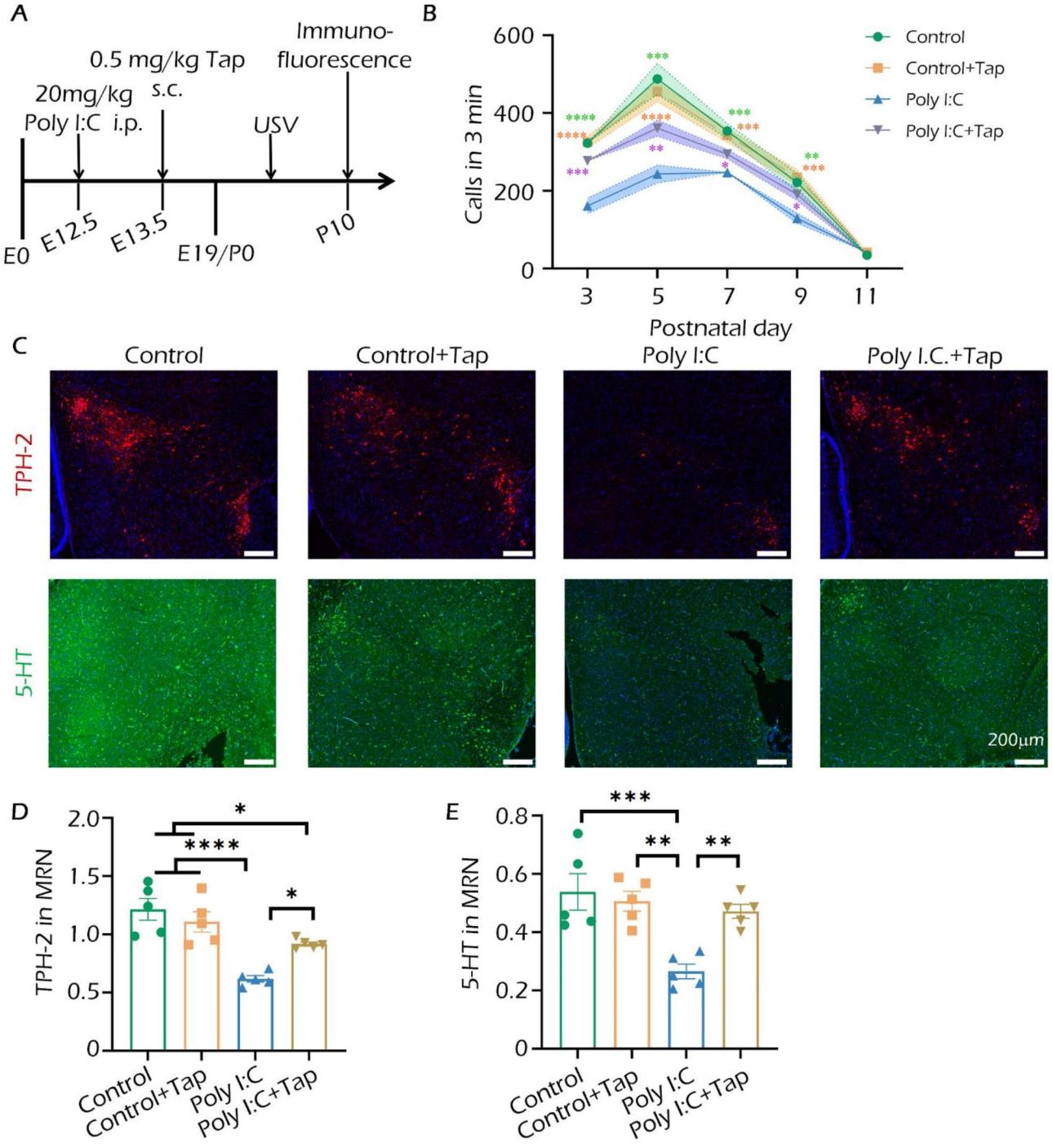

Fig. 7 Taprenepag improved USVs and damage to TPH-2$^+$ neurons in offspring exposed to poly(I: C). (**A**) The total number of calls for newborn pups in 3 min in the isolation-induced distress vocalization assay. ($n = 12$, "n" represents offspring from different dams). Pregnant mice received 20 mg/kg poly(I: C) at E12.5 and taprenepag treatment (0.5 mg/kg). USV was conducted on P3-P11, regardless of gender. (**B**) and (**C**) The mean fluorescence intensity of immunofluorescence staining for TPH-2$^+$ (**B**) and 5-HT (C) in the MRN of newborn pups. ($n = 5$ dams, respectively). (**D**) Immunofluorescence staining of TPH-2$^+$ neurons and 5-HT in newborn MRN pups at P10. Statistics were calculated by one-way ANOVA with Dunnett's post hoc test for (**D**) and (**E**) and two-way ANOVA with Tukey's post hoc test for (**B**). Statistical significance was denoted by $^*P < 0.05$; $^{**}P < 0.01$; $^{***}P < 0.001$; $^{****}P < 0.0001$. The graphs show the mean ± SEM

calculated as the ratio of the Gd content in the placenta or fetus to the Gd content in the maternal blood.

The ultrastructures of Tjs in placental syncytiotrophoblast cells (SVTs) were observed by TEM [10, 33, 40]. And ultrastructures of the innermost epithelial layer was observed by SEM with a Nova Nano 450 microscope (Thermo FEI, Chech) [41, 42]. See supplementary methods.

Pregnancy studies

At E14.5, maternal blood was collected and the total white blood cell concentration (WBC, 10^9/L) and the percentages of each immune cell in pregnant mice were analyzed by an automatic blood analyzer (TEK8500, TECOM SCIENCE, Shenzhen, China). Macroscopic evaluation was conducted for all placental-fetal units (E14.5) in the uterus to identify viable or reabsorbed fetuses. Prevalence of fetal resorption (%) was defined as the percentage of pregnant mice with any (at least one) fetal resorption event [8]. The number of abortive pregnant females and normal pregnant females was analyzed by a two-tailed χ2 test. Fetuses resorbed per mother (%) were expressed as the percentage of the resorbed fetuses in total fetuses. See supplementary methods.

Cell–cell communication analysis

The single-cell expression-count data with cell classifications used droplet-based data (E-MTAB-6701) from a previous publication [43]. The cell-cell communication networks were assessed by the public analysis tool CellPhoneDB [44], which identifies potentially relevant interactions between cell types based on cell type-specific receptor–ligand interactions. See supplementary methods.

Isolation of placental cells and flow cytometry

Twenty-four hours after drug treatment in VPA-exposed pregnant mice, the placentas (E14.5) were prepared as single-cell suspensions, labeled with antibodies, and subsequently analyzed using flow cytometry [43, 45]. Flow cytometry was performed with a CytoFLEX LX (Beckman Coulter, Brea, CA, USA), and the results were analyzed with CytExpert software. See supplementary methods.

Determination of Trp, Kyn, 5-HT and PGE2 levels

Trp: At E14.5, placentas were isolated and immersed in lysis buffer (50 mM Tris·HCl, pH 7.5, 150 mM NaCl, 4 mM $CaCl_2$, 1.5% Triton X-100, and protease inhibitors) according to previous methods [46, 47]. Tissue homogenate solutions were analyzed by high performance liquid chromatography combined with ultraviolet and visible spectrophotometry (HPLC-UV) to determine placental Trp abundance. Kyn: The placental Kyn abundance was quantified using previously reported Ehrlich reagents [48]. 5-HT in placental or fetal brain (E14.5) homogenate solution was quantified by a 5-HT enzyme-linked immunosorbent assay (Enzyme-linked Biotechnology, Shanghai, China) according to the manufacturer's instructions [49]. The PGE_2 level in the placenta homogenate solution was quantified with a PGE_2 ELISA Kit (R&D Systems, Minneapolis, MN, USA) according to previously reported methods [50, 51]. The results of Trp, Kyn, 5-HT and PGE_2 abundance were expressed as the ratio of the measured amount and tissue total protein. See supplementary methods.

VPA assay of JEG-3 cells

To study the direct destructive effect of sodium valproate (VPA) on the Tjs of placental trophoblast cells, JEG-3 cells (P6) were incubated with low dose VPA (7 μg/ml) and high dose VPA (21 μg/ml) for 48 h. Later, the cells were lysed with RIPA lysis buffer and phenylmethanesulfonylfluoride (Beyotime) at 4 ℃ and homogenized for subsequent Western-Blot analysis experiments. The dosage of VPA was determined from unbound serum concentrations of VPA in pregnant women. The low dose was calculated from the average serum concentrations of pregnant women (411 μmol/L) and 90% of the serum proteins bound to VPA [52, 53].

Western blot analysis

Protein expression levels in the placenta (E14.5) were analyzed by WB. The primary antibodies used were as follows. β-actin (Multi sciences; Hangzhou, China; ab36861), β-tubulin (Cell Signaling Technology; Danvers, MA, USA; 2146), claudin-4 (Abcam; Cambridge, UK; ab53156), claudin-5 (Invitrogen; Carlsbad, CA, USA; 35-2500), occludin (Invitrogen; 71-1500), TPH-1 (Abcam; ab52954), PTGER-2 (Abcam; ab167171), COX-2 (Cell Signaling Technology; 12282), IDO-1 (Rockland; ME, USA; 200-301-E57S) and Arg-1 (Proteintech; Wuhan, China; 16001-1-AP). See supplementary methods.

Immunofluorescence or immunohistochemistry

The placentas (20 μm thick) and brains of fetuses (E14.5) (10 μm thick), mouse pups (P10) and adolescent male progeny (P55) (40 μm thick) were sectioned. The primary antibodies used were as follows: TPH-2 (Abcam; ab184505), IDO-1 (Rockland; ME, USA; 200-301-E57S), Netrin-G1a (R&D Systems; Minneapolis, MN, USA; AF1166) and serotonin (Sigma–Aldrich; St Louis, MO, USA; S5545). See supplementary methods.

Behavioral studies

From P3–P54, mice underwent a battery of behavioral tests conducted in the following order [31]: neonatal vocalizations (P3-P11, regardless of gender) [54], open

field testing (P45, male) [55], self-grooming (P48, male) [56], marble burying (P51, male) [57] and three-chamber social interaction (P54, male) [58, 59]. See supplementary methods.

Statistical analysis

All data analysis and figure generation were conducted with GraphPad Prism (7.0). The data are presented as individual data points, and the column chart represents as the mean ± SEM. In all the experiments, "n" represented dams or offspring from different dams. One-way ANOVA with Dunnett's post hoc test was used to assess the differences among three or more groups with only one variable. Comparisons of two or more groups with time variables were assessed by two-way repeated-measures ANOVA with Bonferroni's post hoc correction. A two-tailed χ2 test was used to analyze the prevalence of resorbed fetuses. Differences were considered significant when the P value of the data was less than 0.05. The statistical significance was denoted by ns, not significant; $^{*}P<0.05$; $^{**}P<0.01$; $^{***}P<0.001$; $^{****}P<0.0001$.

Results

VPA exposure during pregnancy disrupted the maternal-fetal barrier and immune homeostasis

A low dose of RU486 (a glucocorticoid antagonist) was reported to increase the expression of placental tight junction proteins and reduce MFB permeability [35]. MRI revealed increased leakage of Gd in VPA-exposed fetuses and decreased leakage of Gd in fetuses of group VPA + RU486 (Fig. 1B and C). Quantitative analysis of Gd revealed 40.5% increased leakage of Gd from maternal blood to the fetus or placenta in pregnant mice exposed to VPA, which was almost completely prevented by the administration of the glucocorticoid antagonist RU486 (Fig. 1D and E). WB results revealed a significant decrease in the expression of Tjs claudin-4 and claudin-5 in the VPA-exposed placentas and RU486 administration increased the Tjs expression (Fig. 1F, H and I). TEM analysis further examined the ultrastructure of Tjs in placental syncytiotrophoblast cells (SCTs) (Fig. 1F). In the control and VPA + RU486 groups, Tjs in the first SCT layer and between inner SCT layers were densely arranged, with membranes completely attached. Conversely, the VPA group showed loosely bound Tjs and large gaps. SEM images of tight junction complexes in the innermost epithelial layer in the VPA group were gradually disrupted, making it difficult to distinguish boundaries between epithelial cells (Fig. 1J). However, this disruption improved after RU486 treatment. These findings suggest that exposure to VPA during pregnancy can severely disrupt the MFB, while RU486 treatment can prevent damage to the MFB.

The study delved into the disruption mechanism of MFB and investigated the impact of RU486 intervention. The expression of Tjs (claudin-4 and occludin) in placental trophoblast JEG-3 cells did not change upon direct exposure to low or high doses of VPA (Figure S1). However, we clearly observed damage to the maternal-fetal barrier function in pregnant mice exposed to VPA. These findings suggested that VPA alone is not sufficient to harm the Tjs of placental trophoblast cells. And it prompted that the damage to placental TJs caused by VPA may involve the interaction with other cells.

Further investigations were conducted to identify the cell types that interact most closely with barrier cells, as well as to examine how these cells are altered in mice exposed to VPA during pregnancy. The cell-cell communication network at the human maternal–fetal interface was analyzed by the tool CellPhoneDB (Figure S2A). The results indicated that decidual macrophages exhibited the closest interactions with fetal barrier cells, followed by decidual NK cells and T cells (Figure S2B). The results of a blood routine examination indicated that maternal blood immune function was disrupted in pregnant mice exposed to VPA. This was evidenced by a significant decrease in total white blood cell concentrations (4.78×10^{9} /L compared to 13.52×10^{9} /L in the control group, as shown in Figure S2C). Furthermore, there were notable changes in the percentages of lymphocytes and monocytes in the blood of VPA-exposed pregnant mice (Figure S2D and Table S1). Placental flow cytometry analysis in Figure S3B and S3C revealed a significant decrease in the percentages of dM and dNK cells in VPA-exposed pregnant mice (12.28% and 10.80%, respectively, compared to 37.79% and 22.10%, respectively, in the control group). Additionally, there was an abnormal increase in the percentage of T cells from 15.43% in normal mice to 37.29% in VPA-exposed mice. These findings suggest that exposure to VPA during pregnancy led to extensive immune disturbance at the maternal-fetal interface, characterized by reduced numbers of dNK and dM cells and hyperactivation of T cells. Moreover, TEM images clearly depicted direct interactions between fetal T cells and fetal endothelial cells, as well as the presence of numerous endothelial cells and SCT cell cavities in fetal vessels (Figure S3D). Similar cavities were observed between SCT cells and dNK cells in the maternal blood sinus (Figure S3E). Overall, the data indicate that VPA exposure during pregnancy resulted in a weakening of the regulatory immune response at the maternal-fetal interface, contributing to the impairment of maternal-fetal barrier function.

Taprenepag upregulated placental IDO-1 and restored homeostasis at the MFI

Subsequent experiments were conducted to investigate the underlying causes of immune disorders at the maternal-fetal interface and to determine appropriate interventions. An imbalance in Trp metabolism was observed in placentas exposed to VPA through the examination of the expression of two key metabolic enzymes, IDO-1 and TPH-1 (Fig. 2B). Specifically, there was a significant downregulation of placental IDO-1, without change in the expression of TPH-1 (Fig. 2C and D). Treatment with RU486 resulted in an upregulation of IDO-1 expression. Given that IDO-1 and its metabolic substrate, Kyn, play a crucial role in maintaining immune tolerance, efforts have been made to enhance IDO-1 expression in order to restore homeostasis at the maternal-fetal interface. Various approaches have been utilized to upregulate IDO-1 expression in order to restore placental immune homeostasis following exposure to VPA (Fig. 2E). Kyn, an aryl hydrocarbon receptor agonist, has been shown to induce effector T cell apoptosis and increase IDO mRNA levels in dendritic cells, making it a common treatment for autoimmune conditions [60–62]. Additionally, Butaprost and Taprenepag, which are agonists of the prostaglandin E_2 receptor (PTGER-2), have been found to elevate IDO-1 mRNA levels in myeloid-derived suppressor cells through a COX-2/PGE_2 positive feedback mechanism [63, 64].

After VPA modeling, fetal weight decreased significantly compared to the control group in Figure S7A. The administration of RU486 and Taprenepag (Tap) enhanced the body weight of VPA-exposed fetal mice. Notably, RU486 administration significantly increased the placental weight of VPA-exposed fetal mice in Figure S7B. The results in Fig. 2E and F indicated that treatment with Tap or RU486 significantly increased the expression of IDO-1 in VPA-exposed placenta across all interventions. Moreover, Tap and Kyn administration partially restored the protein expression level of Arg-1, a marker of dM_2 (Fig. 2E and G). These findings suggest that elevated placental IDO-1 expression may help rebalance the immune system at the MFI after VPA exposure. Additionally, the levels of Tjs claudin-4 and claudin-5 in VPA-exposed placentas returned to normal after RU486 or Tap treatment (Fig. 2H, I and J). In summary, administration of RU486 or Tap can alleviate the MFB disruption at the MFI in VPA-exposed pregnant mice by increasing placental IDO-1 expression.

The following study primarily focused on investigating specific signaling pathways known to regulate placental IDO-1. Prior research has suggested the existence of a positive feedback loop involving COX-2/PGE_2/PTGER-2/IDO-1, which plays a role in maintaining intrinsic immune resistance in human tumors or tumor-associated immunosuppressive cells [63, 64]. The research examined the regulatory effects of RU486 and Tap on the aforementioned pathways. Results indicated a clear inhibitory impact on the COX-2/PGE_2/PTGER-2 positive feedback loop in the placentas of pregnant mice treated with VPA (Fig. 2K, L and P). Specifically, RU486 treatment led to an increase in both inactive and hypoglycosylated COX-2 precursor forms (66 and 70 kDa), as well as active and hyperglycosylated mature COX-2 (72 and 74 kDa) in Fig. 2K, N and O. And the VPA + Tap group only showed elevated levels of glycosylated COX-2. Furthermore, both RU486 and Tap were found to enhance the expression of PGE_2 and PTGER-2 in the placentas of VPA-exposed pregnant mice in Fig. 2L, M and P. These findings suggest that RU486 and Tap may upregulate placental IDO-1 expression by amplifying the COX-2/PGE_2/PTGER-2 positive feedback loop.

The experiments investigated the impact of VPA exposure on placental Trp metabolism and placental immune system and the effectiveness of drug intervention. VPA exposure reduced placental Kyn abundance and increased Trp abundance due to the downregulation of placental IDO-1 (Fig. 3B and C), hindering Trp metabolism via the Kyn pathway. Additionally, 5-HT levels in the placentas and fetal brains rose significantly after VPA exposure (Fig. 3D, F, H and E). Treatment with RU486 or Tap reversed the imbalance in placental Trp metabolism caused by VPA exposure. Flow cytometry analysis further demonstrated that the immune disorder at the MFI induced by VPA exposure was reversed by RU486 or Tap treatment, leading to increased percentages of dM and dNK cells and decreased T cell percentage (Fig. 3G and I). Subsequent investigations confirmed that RU486 and Tap decreased the VPA-induced rise in dM_1 cell numbers and restored dM_2 cell numbers (Fig. 3J and K). In summary, administration of RU486 or Taprenepag can alleviate the MFB disruption and the abundance of placental immune cells at the MFI in VPA-exposed pregnant mice by modulating placental IDO-1 expression.

Taprenepag promotes the development of serotonergic neuronal systems in fetuses exposed to VPA

We next investigated the impact of elevated serotonin (5-HT) levels in the fetal brain on the development of serotonergic neuronal systems. The brain's endogenous serotonin is primarily synthesized through Trp hydrolysis by tryptophan hydrolase 2 (TPH-2) in serotonergic neurons. Serotonergic neurons appeared in the raphe nuclei (RN) and were generated in early development at embryonic days (E10.5–E12.5). These axon tracts partially passed through the midline of the rhombencephalon, gradually extended to the dorsal thalamus (DT) and hypothalamus and eventually projected into the cortex until birth (Fig. 4A) [65, 66].

Our findings revealed a notable reduction in the number of serotonergic neurons in the dorsal raphe (DR) and median raphe nuclei (MRN) at E14.5 in fetuses exposed to VPA (Fig. 4B). Consequently, fewer axon tracts of serotonergic neurons expressing TPH-2 extended ventrally into the forebrain through the medial forebrain bundle (MFB), as shown in Fig. 4C. Treatment with Tap partially mitigated the decrease in TPH-2^+ neurons induced by VPA, showing superior efficacy compared to RU486. However, neither Tap nor RU486 treatment significantly improved the axon tracts of TPH-2^+ neurons in the MFB, revealing the continued retardation of TPH-2^+ neuron development. Subsequent studies were carried out to evaluate the development of corticocollicular neurons and posterior thalamocortical axons (TCAs), whose development are regulated by TPH-2^+ neuron in the RN. The immunoreactivity of Netrin-G1a, a marker of developing thalamocortical axons, was reduced in the ventral pallidum (VP) of fetal brains exposed to VPA, resulting in the absence of longer Netrin-G1a$^+$ axon bundles (Fig. 4D) [67]. Moreover, there was a decrease in positive TCAs in the internal capsule (IC) in the VPA group compared to the control group, while the number of Netrin-G1a$^+$ axon bundles in the caudate putamen (CP) remained relatively stable. Although RU486 partially restored the number of TCAs in the dorsal thalamus (DT), TCAs in IC and CP exhibited dysplasia with limited axon bundle formation. Treatment with Tap not only enhanced the formation of TCAs in DR but also facilitated the passage of TCA projections through IC and CP. These findings collectively suggest that fetal brain subjected to elevated 5-HT levels in the VPA model exhibited impaired development of the serotonergic neuron system, characterized by damage to serotonergic neurons and degeneration of TCAs. Tap treatment promoted the development of serotonergic neuronal systems in fetuses exposed to VPA.

Taprenepag treatment improved ASD-related behavioral abnormalities in VPA-exposed offspring

Previous research has indicated that exposure to VPA during pregnancy may lead to behavioral abnormalities associated with ASD in offspring [31]. We further investigated the effects of Taprenepag treatment at varying doses during pregnancy on general activity, anxiety-like behaviors, repetitive stereotyped behaviors, and social behaviors in VPA-exposed offspring. Morphological analysis of embryos at E14.5 revealed that Tap treatment significantly reduced prevalence of abortion in pregnant mice and fetal resorption rates when compared to VPA or RU486 treatments (Fig. 5B C). Communication deficits in VPA-exposed offspring were assessed through neonatal ultrasonic vocalization (USV) calls at multiple time points. Pups exposed to VPA emitted fewer vocalizations post-separation from mothers, indicating communication deficits (Fig. 5D). However, both low and high doses of Tap treatment led to an increase in USV calls, suggesting an improvement in communication tendencies. Locomotion and anxiety-like behavior were assessed by open field exploration at P45. VPA-exposed offspring exhibited increased anxiety with less time spent in the center of the testing arena (Figure S6A). Tap treatment did not effectively alleviate anxiety symptoms. Locomotion did not significantly differ between VPA-exposed and control offspring (Figure S6B). VPA-exposed offspring also exhibited heightened marble burying-elicited stereotyped behaviors and increased self-grooming behaviors compared to normal pups (Fig. 5E and F and S5C). A low dose of Tap was more effective in alleviating repetitive stereotyped behaviors in VPA-exposed offspring than a high dose of Tap.

Three-chamber social interaction tests were performed to assess social behaviors. In the sociability test, offspring exposed to VPA showed a preference for interacting with a novel object over a new mouse, unlike the control group (Fig. 5G and S5D). Both low and high doses of Tap were found to improve social deficits in VPA-exposed offspring, as evidenced by their preference for the mouse chamber. In social recognition testing, offspring in the control or VPA + Low Tap group favored interaction with an unfamiliar mouse rather than a familiar one (Fig. 5H and S5E). Conversely, offspring in the VPA and VPA + High Tap groups displayed an ambiguous preference for both chambers, suggesting that a high dose of Tap was not effective in restoring social discrimination ability. Overall, administering a low dose of Tap during pregnancy improved communication skills, reduced repetitive stereotyped behaviors, and enhanced social interactions in VPA-exposed offspring based on the results of these behavioral tests.

Following behavioral testing, the study examined the levels of TPH-2 and 5-HT in the RN to establish connections between ASD-related behavioral abnormalities and serotonergic neurons. The research revealed a noticeable reduction in TPH-2^+ neurons in the DR and MRN of VPA-exposed offspring (Fig. 5I, J, K and L), consistent with the findings in fetal brains at E14.5 (Fig. 4D). Moreover, there was a significant decrease in 5-HT levels in VPA-exposed offspring, attributed to reduced TPH-2 expression. Consequently, the study linked ASD-related behavioral abnormalities in VPA-exposed adolescent offspring to impairments in serotonergic neurons. Interestingly, Tap treatment during pregnancy was found to restore the number of TPH-2^+ serotonin neurons and 5-HT levels in the raphe nuclei of offspring, leading to improved performance in behavioral tests.

Inhibition of placental IDO-1 antagonized the therapeutic effect of tap

To investigate whether Tap's effect on autism treatment is linked to placental IDO-1 regulation, Tap's therapeutic impact was further evaluated in combination with the pharmacological inhibitor linrodostat (Lin), an irreversible IDO-1 inhibitor. Administering Lin alone during pregnancy did not notably alter fetal weight or placental weight at E14.5 (Figure S7C and S7D). However, fetal weight significantly increased following Tap treatment compared to VPA treatment alone (Figure S7C). Interestingly, this increase in fetal weight induced by Tap was attenuated by coadministration of Tap and Lin. Examination of placental IDO-1 expression levels revealed that IDO-1 expression decreased in VPA-exposed placentas compared to the control group (Fig. 6B and C). Moreover, Tap administration elevated IDO-1 expression in VPA-exposed placentas, which was counteracted by Lin. Maternal blood routine examination indicated WBC in VPA-exposed pregnant mice was improved after Tap treatment, in contrast to that in mice coadministered Lin (Figure S8A and S8B). MFB integrity was assessed through morphological evaluation of Tjs in both the amniotic epithelium and placental syncytiotrophoblast layers. In the Tap group, the tight junction complexes in the amniotic epithelium exhibited close connections with clear cell boundaries (Fig. 6D). Conversely, coadministration of Lin resulted in sparse and separate tight junction complexes. The ultrastructure of Tjs in placental syncytiotrophoblasts was dense and numerous in the Tap group (Fig. 6E), while in the VPA + Tap + Lin group, they were loosely bound and disrupted, resembling the observations in the VPA group. These findings suggest that the protective effects of Tap on the MFI were attributed to the upregulation of placental IDO-1, which was hindered by the irreversible IDO-1 inhibitor linrodostat.

The subsequent ASD-related behavioral abnormalities in the offspring were evaluated by isolation-induced distress vocalizations (Fig. 6F). Offspring from the VPA and VPA + Lin groups displayed reduced willingness to communicate upon separation from their mothers. Tap increased ultrasonic vocalizations and improved social deficits in VPA-exposed pups. However, the anti-autism effect of Tap was reversed after IDO-1 inhibition by Lin. The development of serotonergic neurons was examined histopathologically in pups at P10. Pups exposed to VPA showed decreased immunoreactivity of TPH-2^+ and lower 5-HT levels in the RN. Treatment with Tap mitigated VPA-induced damage to serotonergic neurons (Fig. 6G and H, and 6I). The therapeutic effect of Tap on serotonergic neurons was hindered by Lin administration. Overall, Tap's effect on autism treatment were found to be mediated by IDO expression regulation and could be counteracted by an IDO-1 inhibitor.

Taprenepag treatment improved neurodevelopmental disorders in MIA-exposed offspring

In a maternal inflammation model (MIA) induced by poly(I: C) exposure during pregnancy, disturbances in tryptophan metabolism in the placenta have been attributed to the overactivation of tryptophan hydroxylase [68]. Additionally, fetal mice exhibited delays in the 5-HT-dependent neurogenesis process and demonstrated neurodevelopmental disorders (NDDs). We further investigated the therapeutic effects of Tap on NDDs in offspring mice within this model. Tap treatment resulted in increased ultrasonic vocalizations and improved social deficits in pups subjected to MIA (Fig. 7A). Furthermore, MIA-exposed pups exhibited decreased immunoreactivity of TPH-2^+ and lower 5-HT levels in the RN (Fig. 7C and D, and 7E). In contrast, Tap treatment enhanced the immunoreactivity of TPH-2^+ and elevated 5-HT levels compared to pups subjected to poly(I: C). Notably, no significant changes were observed in ultrasonic vocalizations, TPH-2 positivity, or serotonin positivity in the RN of mice that received a single administration of Tap when compared to the control group. These findings suggest that a single administration of Tap during pregnancy did not lead to significant neurotoxicity in mouse pups.

Discussion

IDO-1 catalyzes the oxidation of Trp to kynurenine, a process that exerts its biological effects through local Trp depletion and/or the accumulation of kynurenine metabolites. In the human placenta, IDO-1 is expressed in endothelial cells, syncytiotrophoblasts, extravillous trophoblasts, stromal cells, and macrophages [69]. The potential consequences of IDO1-mediated L-tryptophan catabolism in the endothelium include antimicrobial activity, immunosuppression, and relaxation of placental vasotonus, contributing to placental perfusion and the growth of both the placenta and fetus [22].

Decreased expression of IDO-1 in the placenta has been extensively documented in both human patients and mouse models. Placentas from patients experiencing pre-eclampsia, intrauterine growth restriction, or recurrent miscarriage exhibit reduced levels of placental IDO-1 mRNA, protein, and Trp-degrading activity [70–72]. Notably, the lower IDO-1 activity is associated with more severe maternal hypertension or proteinuria [70]. IDO1-deficient mice exhibit pre-eclampsia-like symptoms during gestation, including elevated blood pressure, litter size and significant fetal weight loss, although this deficiency does not impact fecundity [73]. In allogeneic pregnancies in mice, pharmacological inhibition of IDO1 results in T cell-mediated hemorrhagic necrosis and rejection of the conceptus shortly after implantation [74, 75]. Additionally, these pregnant mice develop hypertension and proteinuria alongside localized circulation

impairment in the placenta, mirroring the lesions characteristic of human pre-eclampsia [76].

As mentioned above, IDO-1 deficiency is implicated in various human pregnancy-related disorders. Consequently, identifying a treatment method that can upregulate IDO-1 expression holds significant clinical value. As detailed in our study, we have demonstrated that Tap can enhance placental IDO-1 expression, restore immune homeostasis at the maternal-fetal interface in VPA-exposed pregnant mice, and ameliorate neurodevelopmental disorders in fetal mice. This finding also suggests potential applications in the treatment of other disease models characterized by IDO-1 deficiency.

Taprenepag is an agonist for the prostaglandin E2 receptor (EP2), used in clinical trials phase 2 for the treatment of Ocular Hypertension and Glaucoma, Open-Angle. Taprenepag was found to be well tolerated at 10 μg and 30 μg doses in rabbits, 10 μg in dogs and monkeys and 0.81 μg in human following topical ocular dosing [77]. The most frequently reported ocular adverse events in humans were conjunctival hyperemia (Stage I, 13/67 [19.4%]; Stage II, 83/250 [33.2%]) and photophobia (Stage I, 9/67 [13.4%]; Stage II, 52/250 [20.8%]) [79]. In preclinical research, EP_2 receptor agonists exhibit various biological activities, including ocular hypotension, tocolysis, and anti-inflammatory effects [79]. The therapeutic indications for EP2 agonist therapy aimed at alleviating smooth muscle spasms have been recognized for over three decades. These indications encompass tocolysis for the prevention of preterm labor and the management of dysmenorrhea [80]. EP2 receptors facilitate uterine quiescence and inhibit uterine contractions via the intracellular adenylyl cyclase and cAMP signaling pathway, thereby preventing the termination of pregnancy and preterm labor [81, 82].

In our research, we evaluated the neurotoxicity of a single Tap administration on fetal mice in Fig. 7. The results indicated that, compared to the control group, single Tap administration did not affect the expression of Tph-2 and 5-HT in serotonin neurons within the raphe nucleus of mouse pups, nor did it impact the number of ultrasounds in these mice. These findings suggest that single Tap administration during pregnancy does not result in significant neurotoxicity in mouse pups.

The observation that low-dose Tap is more effective than high-dose Tap lacks substantial experimental support, and this phenomenon is indeed challenging to elucidate. However, we concur with one possible explanation. Both this study and previous research have highlighted that placental tryptophan metabolism serves as the important regulatory pathway for maintaining homeostasis at the maternal-fetal interface. Tryptophan can be oxidized to kynurenine by IDO-1 in the placenta, which is essential for sustaining placental immune tolerance. Concurrently, tryptophan can also be hydroxylated to serotonin by TPH-1, a process that is crucial for regulating fetal neurodevelopment. Achieving a balance between these two pathways is critical for the normal development of the fetus. We hypothesize that administering excessively high doses of Tap may lead to an overactivation of IDO-1 expression, consequently inhibiting the TPH-1/5-HT pathway. This inhibition could be detrimental to fetal neurological development. Therefore, in this study, low-dose Tap proved to be more effective in addressing fetal neurodevelopmental disorders induced by VPA.

Mifepristone (RU486) is a synthetic steroid antagonist with a strong antagonism to progesterone (P4), glucocorticoid receptor (GR) and, to a lesser extent, to the androgen receptor (AR). Mifepristone is an effective drug for termination of early pregnancy. However, various results demonstrate that the dosage and the application time of Mifepristone are closely associated with abortion rates. Generally speaking, it is generally believed that mifepristone has no clear embryotoxicity in rodents at doses below 0.5 mg/kg [83]. For example, Zhu et al. applied 1.20, 0.40, and 0.20 mg Mifepristone/kg BW to mice on Pd4, Pd8, and Pd12, respectively, and found that these strategies did not affect pregnancy rates and litter sizes of mice [84]. RU486 (0.025–0.1 mg/kg) showed no activity on early pregnancy termination for rats on the day gestation of 13-15 [85]. In this study, the administered dose of RU486 was only 0.05 mg/kg, significantly lower than the doses reported in the literature that are known to induce embryo resorption. Consequently, the likelihood of RU486 causing embryonic abortion in this study is considered negligible. In this study, we hypothesize that the protective effects of RU486 on the maternal-fetal barrier and the regulation of maternal-fetal interface immunity may be associated with its antagonism of glucocorticoid-induced increases in COX-2/PEG2/IDO-1, rather than its antagonism of progesterone-mediated abortion. The reasons are as follows.

Low dosage of RU486 was observed to regulate the immune alterations of the maternal-fetal interface. Progesterone was observed to decrease in vitro IDO expression in dendritic and $CD4^+$ cells from maternal-fetal interface of rats. And the blocking of progesterone receptor on these cells by mifepristone restored IDO expression levels [86]. And low dosage of Mifepristone treatment (0.8 mg/kg) in mice at 14.5 day of pregnancy was observed to increase the expression of Gal-9 in decidual Treg, $CD4^+$T cells and Th cells. Gal-9 is an important role in the regulation of maternal immune tolerance [87]. Treated with 2.5 μg/mouse of RU486 (about 0.06 mg/kg) for mice on P15 was reported to increase the expression of claudin-4 mRNA and protein [35]. In summary, the likelihood of embryonic abortion resulting

from low doses of RU486 is minimal, and its protective effect on the maternal-fetal interface can be explained. This effect is associated with the restoration of immune homeostasis, which is attributed to the upregulation of IDO-1.

In this research, we observed a disruption of the maternal-fetal barrier and an impairment of the development of the serotonergic neuronal system in VPA-exposed mice. Although the study lacks direct evidence demonstrating that excess 5-HT from the placenta permeates the fetus through a compromised maternal-fetal barrier, we contend that the disruption of the maternal-fetal barrier may exacerbate the 5-HT-dependent neurogenic processes in the fetal RN, potentially leading to neurodevelopmental disorders in fetal mice. The rationale for this assertion is as follows.

(1) Excessive serotonin affects the development of serotonergic neuron system in fetal mice. It has been reported that 5-HT plays a role in altering the attraction exerted by netrin-1 on TCAs in the developing mouse brain, shifting it from attraction to repulsion. Excessive 5-HT levels resulting from the knockout of the serotonin transporter (SERT) have been found to affect the patterning of thalamic axons and the structure of cortical neurons, leading to neurodevelopmental disorders and anxiety-like behaviors in mice. Overproduction of 5-HT has been associated with fetal neurodevelopmental disorders mediated by maternal inflammation activation.

(2) The sources of 5-HT in the fetal forebrain and hindbrain are regulated by two distinct sets of mechanisms, with their dominant contributions shifting as the embryo develops. In the hindbrain, 5-HT primarily originates from the metabolism of tryptophan by Tph-2^{+} serotonergic neurons. However, in the forebrain at early ages (E10.5 to E15.5), it predominantly derives from tryptophan metabolism by Tph-1 in the placenta. After E16.5, forebrain 5-HT becomes exclusively provided by DR serotonergic neurons with raphe axons reaching the forebrain [88, 89].

(3) Other pathways for 5-HT production were excluded. Between embryonic days 10.5 and 15.5, the fetal intestine lacks the synthetic capacity to produce serotonin. Furthermore, 5-HT from maternal blood is unable to cross the placental barrier to enter the fetus. While the blood and platelets of maternal SERT knockout (SERT$^{-/-}$) mice lack 5-HT, the serotonin (5-HT) content in the fetal forebrain is comparable to that of wild-type mice in SERT knockout (SERT$^{+/-}$) fetal mice. Additionally, Bonnin et al. employed ex vivo mouse live placental organ perfusion technology, revealing that significant amounts of fresh 5-HT could be collected in the umbilical artery and vein only when perfusing tryptophan-containing solution from the uterine artery. In contrast, infusing 5-HT alone resulted in the collection of less than 1% of 5-HT [88, 89].

(4) The blood-brain barrier in fetal mice is generally understood to begin forming at E15. This process is characterized by the coverage of endothelial capillary walls by pericytes, which is accompanied by a restriction of intercellular blood flow and the emergence of perivascular structures [34]. Our studies on fetal mouse neurodevelopment typically continued until E14.5. At this stage, the blood-brain barrier in the fetal mouse has not yet formed; therefore, it was not considered in our research.

A sound experimental design should employ mouse isolated live placenta perfusion technology to perfuse both normal placentas and those exhibiting compromised barrier function due to VPA modeling with a 5-HT solution. By measuring the differences in 5-HT content within the fetal side vascular outflow fluid, we can directly validate our hypothesis.

Another limitation of this study is the failure to consider the impact of sexual dimorphism on placental function and pregnancy outcomes. An increasing body of evidence indicates that numerous placental functions and disorders exhibit sexual dimorphism. During the formation of the human placenta, trophoblast cells from the extrablastocystic trophectoderm invade the maternal decidua, giving rise to the placenta and chorion. Consequently, the resulting extraembryonic compartment shares the same biological sex as the developing embryo. Sex differences in prenatal development often highlight male vulnerability; male fetuses have been reported to be at a higher risk for early preterm birth, term preeclampsia (PE), placental inflammation, premature rupture of membranes (PPROM), and various other pregnancy complications [90]. Given the observed sex differences in common pregnancy pathologies, the sex of the trophoblast and other cellular components of the placenta may significantly influence the interactions between fetal and maternal cells.

Microarray analyses of placental tissue and isolated placental cell types have revealed significant sexual dimorphism in gene expression within the human placenta. Current studies on early placental development consistently demonstrate sex differences in cell adhesion and cell-cell interactions, making this functional category one of the most prominent and well-defined distinctions in early human placental transcription [90]. Gonzalez et al. identified differential expression of genes related to cell adhesion, ciliogenesis, and intercellular communication (including *OFD1*, *OSBL3*, *PCDH11Y*, and *TBC1D32*) between male and female placentas, indicating gender-based differences in the interactions of placental cells with their environment [91]. Furthermore, Braun et al. reported that female placentas exhibit a greater expression advantage in the extracellular matrix remodeling signaling network, which is centered on bead filament collagens, integrins, laminins, and matrix

metalloproteinase regulatory factors [92]. In addition, other research revealed that male placentas show higher expression levels of pro-inflammatory signals such as TLR4 and TNF-α, while female placentas express higher levels of the LHB-CGB signal cluster, which is advantageous for maintaining immune tolerance [90]. Therefore, we speculate that the maternal-fetal barrier exhibits sexual dimorphism in its capacity to resist external pathogenic factors and to facilitate self-recovery. The stronger expression of cell adhesion signaling networks in female placentas may enhance their self-healing capabilities following damage to the placental barrier, potentially leading to improved pregnancy outcomes. Further experimental validation is necessary to confirm these findings.

Conclusion

Our data demonstrate that the metabolism of L-tryptophan in the placenta plays a crucial role in maintaining the balance at the maternal–fetal interface and supporting fetal neurodevelopment. Specifically, Trp is primarily metabolized in the Kyn pathway by indoleamine 2,3-dioxygenase, contributing to immune tolerance. Moreover, Trp is converted to serotonin through the serotonin pathway by tryptophan hydroxylase 1, which is essential for normal fetal neurodevelopment. Exposure to VPA during pregnancy was found to disrupt the COX-2/PGE_2/PTGER-2/IDO-1 feedback loop, leading to a decrease in IDO-1 levels and subsequent maternal immune activation. This activation was characterized by an increase in T cell population and a shift from dM_2 to dM_1 polarization. Additionally, excessive Trp in the placenta is converted to serotonin, which can cross the MFB and affect the fetal brain, resulting in damage to serotonergic neurons and regression of thalamocortical axons. Treatment with taprenepag (PTGER-2 agonists) during pregnancy was shown to increase IDO-1 expression, restore maternal–fetal interface homeostasis, and mitigate the damage to serotonergic neurons and autism-like behaviors in offspring mice exposed to VPA. The COX-2/PGE_2/PTGER-2/IDO-1 positive feedback loop is crucial for maintaining immune homeostasis and the integrity of the MFB (Fig. 8). Overall, our research suggests a novel therapeutic strategy for promoting healthy fetal neurodevelopment and preventing neurodevelopmental disorders by restoring homeostasis at the maternal-fetal interface.

This work presents a comprehensive analysis of the compromised MFB function in VPA-induced autism, encompassing disruptions in the amniotic epithelium barrier, impairment of placental TJs, and increased permeability of Gd agents. While existing evidence indicates a strong association between placental development disorders and autism, limited research has explored alterations in the MFB in individuals with autism and the interconnection between these conditions. Our findings

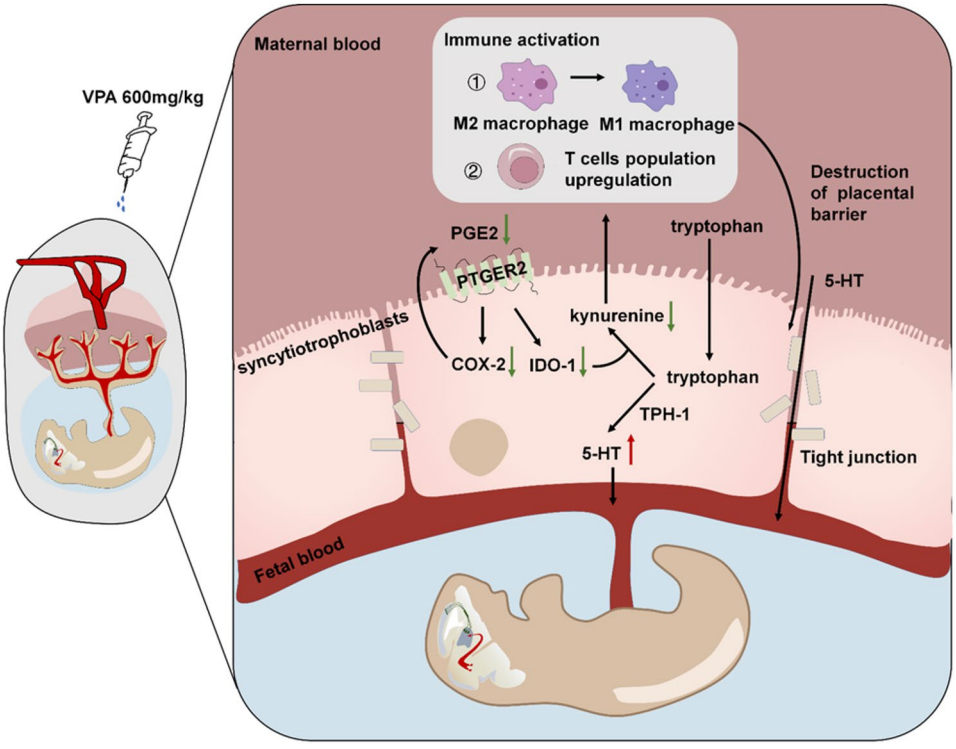

Fig. 8 Taprenepag can restore homeostasis of maternal–fetal interface, improve damage to serotonergic neurons and offspring neurodevelopmental disorders via the activation of feedback loop COX-2/PGE2/PTGER-2

demonstrate that MFB disruption results in elevated serotonin levels in the fetal brain in VPA-induced autism, leading to damage to serotonergic neurons and neurodevelopmental deficits. The impairment of the MFB may serve as a significant causal factor or a common comorbidity of autism. Non-invasive and minimally invasive prenatal assessments of MFB integrity in expectant mothers can aid in the identification and diagnosis of non-hereditary autism in fetuses. Furthermore, our study offers insights for early intervention in autism and potentially for the management of fetuses at risk of neurodevelopmental disorders.

Abbreviations

NDDs	Neurodevelopmental disorders
MFI	Maternal–fetal interface
IDO-1	Indoleamine 2,3-dioxygenase
VPA	Valproate
ASD	Autism spectrum disorders
MFB	Maternal-fetal barrier
Trp	L-tryptophan
Kyn	Kynurenine
5-HT	5-hydroxytryptamine or serotonin
SERT	Serotonin transporter
dNK	decidual natural killer cells
dM	decidual macrophages
TPH-2	Tryptophan hydroxylase 2
TEM	Transmission electron microscopy
SCTs	Syncytiotrophoblast cells
Tjs	Tight junction proteins
COX-2	Cyclooxygenase-2
USV	Ultrasonic vocalization
MRN	Median raphe nuclei

Supplementary Information

The online version contains supplementary material available at https://doi.org/10.1186/s12974-024-03300-7.

Supplementary Material 1: Supporting Information I includes semi-quantification of the Western blot or immunofluorescence, gating strategy for flow cytometric clustering, the cell-cell communication networks, fetal weight and placental weight, immune cells analysis in maternal blood and behavioral evaluation and detailed experiment protocols.

Supplementary Material 2: Supporting Information II includes raw images of the Western-blot, immunofluorescence, flow cytometric clustering and MRI images

Acknowledgements

The authors would like to thank Jingyao Chen and Qiong Huang from the Core Facilities, Zhejiang University School of Medicine for their technical support with the histology and immunochemistry analysis. The authors would like to thank Beibei Wang and Dandan Song from the Center of Cryo-Electron Microscopy (CCEM), Zhejiang University, for their technical support in sample preparation and imaging for TEM and SEM. The authors would like to thank Professor Daishun Lin and colleague Zeyu Liang for their technical support to magnetic resonance imaging. The authors would like to thank Professor Xiangnan Zhang for the advice on the writing and review of this manuscript.

Author contributions

Kai Wang: Conceptualization, Methodology, Formal analysis, Investigation, Data curation, Writing - Original Draft, Writing – Review & Editing. Shufen Zhang: Methodology, Formal analysis, Investigation, Data curation, riting - Original Draft, Writing – Review & Editing. Yunxia Wang: Methodology, Formal analysis, Writing – Review & Editing. Xiaomei Wu and Lijun Wen: Methodology, Formal analysis. Tingting Meng and Xiangyu Jin: Data curation, Writing - Original Draft. Sufen Li, Yilin Hong and Yichong Xu: Writing - Original Draft, Writing - Review& Editing. Hong Yuan: Resources, Supervision, Project administration, Funding acquisition. Fuqiang Hu: Conceptualization, Resources, Writing - Review & Editing, Supervision, Project administration, Funding acquisition.

Funding

This work was supported by the National Natural Science Foundation of China (81973267) and the Zhejiang Provincial Natural Science Foundation of China (D19H300001F).

Data availability

Data is provided within the manuscript or supplementary information files.

Declarations

Ethics approval and consent to participate

All pregnant mice and offspring were bred and maintained in specific pathogen-free barrier facilities, and all procedures were approved and conducted according to the guidelines established by the ethics committee of Zhejiang University.

Consent for publication

Not applicable.

Competing interests

The authors declare no competing interests.

Received: 12 June 2024 / Accepted: 16 November 2024
Published online: 28 November 2024

References

1. Michaelson SD, Ozkan ED, Aceti M, et al. SYNGAP1 heterozygosity disrupts sensory Processing by reducing touch-related activity within Somatosensory Cortex circuits. Nat Neurosci. 2018;21(12):1–13. https://doi.org/10.1038/s41593-018-0268-0.
2. Reddihough DS, Marraffa C, Mouti A, et al. Effect of Fluoxetine on obsessive-compulsive behaviors in children and adolescents with Autism Spectrum disorders. Jama-J Am Med Assoc. 2019;322(16):1561. https://doi.org/10.1001/jama.2019.14685.
3. Maenner MJ, Shaw KA, Bakian AV, et al. Prevalence and characteristics of Autism Spectrum Disorder among children aged 8 years - Autism and Developmental Disabilities Monitoring Network, 11 sites, United States, 2018. Mmwr Surveill Summ. 2021;70(11):1–16. https://doi.org/10.15585/mmwr.ss7011a1.
4. Yip BHK, Bai D, Mahjani B, et al. Heritable variation, with little or no maternal effect, accounts for recurrence risk to Autism Spectrum Disorder in Sweden. Biol Psychiat. 2018;83(7):589–97. https://doi.org/10.1016/j.biopsych.2017.09.007.
5. Lord C, Brugha TS, Charman T, et al. Autism spectrum disorder. Nat Rev Dis Primers. 2020;6(1):5. https://doi.org/10.1038/s41572-019-0138-4.
6. Ceasrine AM, Devlin BA, Bolton JL, et al. Maternal Diet disrupts the placenta–brain Axis in a sex-specific manner. Nat Metab. 2022;4(12):1732–45. https://doi.org/10.1038/s42255-022-00693-8.
7. Ander SE, Diamond MS, Coyne CB. Immune responses at the maternal-fetal interface. Sci Immunol. 2019;4(31):eaat6114. https://doi.org/10.1126/sciimmunol.aat6114.
8. Paolino M, Koglgruber R, Cronin SJF, et al. RANK Links Thymic Regulatory T Cells to fetal loss and gestational diabetes in pregnancy. Nature. 2021;589(7842):442–7. https://doi.org/10.1038/s41586-020-03071-0.
9. Choi GB, Yim YS, Wong H, et al. The maternal Interleukin-17a pathway in mice promotes Autism-Like phenotypes in offspring. Science. 2016;351(6276):933–9. https://doi.org/10.1126/science.aad0314.
10. Lu H, Yang H, Zhou W, et al. Rapamycin prevents spontaneous abortion by triggering decidual stromal cell autophagy-mediated NK Cell Residence. Autophagy. 2021;17(9):2511–27. https://doi.org/10.1080/15548627.2020.1833515.
11. Care AS, Diener KR, Jasper MJ, Brown HM, Ingman WV, Robertson SA. Macrophages regulate Corpus Luteum Development during embryo implantation in mice. J Clin Invest. 2013;123(8):3472–87. https://doi.org/10.1172/JCI60561.
12. Arumugasaamy N, Gudelsky A, Hurley Novatny A, Kim PCW, Fisher JP. Model placental barrier phenotypic response to Fluoxetine and Sertraline: a

comparative study. Adv Healthc Mater. 2019;8(18):1900476. https://doi.org/10.1002/adhm.201900476.
13. Afrouzian M, Al-Lahham R, Patrikeeva S, et al. Role of the Efflux transporters BCRP and MRP1 in human placental Bio-disposition of Pravastatin. Biochem Pharmacol. 2018;156:467–78. https://doi.org/10.1016/j.bcp.2018.09.012.
14. Heckmann N, Auran R, Mirzayan R. Application of amniotic tissue in orthopedic surgery. Am J Orthop (Belle Mead NJ). 2016;45(7):E421–5.
15. Santos HP Jr, Bhattacharya A, Joseph RM, et al. Evidence for the Placenta-Brain Axis: Multi-omic Kernel Aggregation Predicts Intellectual and Social Impairment in children born extremely Preterm. Mol Autism. 2020;11(1). https://doi.org/10.1186/s13229-020-00402-w.
16. Vacher C, Lacaille H, O Reilly JJ, et al. Placental endocrine function shapes Cerebellar Development and Social Behavior. Nat Neurosci. 2021;24(10):1392–401. https://doi.org/10.1038/s41593-021-00896-4.
17. Whitaker EE, Johnson AC, Miller JE, Lindner DP, Cipolla MJ. Abnormal development of cerebral arteries and veins in offspring of experimentally preeclamptic rats: potential role in Perinatal Stroke. Mech Ageing Dev. 2021;196:111491. https://doi.org/10.1016/j.mad.2021.111491.
18. Chen Q, Gouilly J, Ferrat YJ, et al. Metabolic reprogramming by Zika Virus provokes inflammation in human placenta. Nat Commun. 2020;11(1). https://doi.org/10.1038/s41467-020-16754-z.
19. Maes M, Anderson G, Betancort MS, Seo M, Ojala JO. Integrating Autism Spectrum Disorder Pathophysiology: Mitochondria, vitamin a, CD38, oxytocin, serotonin and melatonergic alterations in the Placenta and Gut. Curr Pharm Des. 2019;25(41):4405–20. https://doi.org/10.2174/1381612825666191102165459.
20. Bronson SL, Bale TL. The Placenta as a mediator of stress effects on neurodevelopmental reprogramming. Neuropsychopharmacol. 2016;41(1):207–18. https://doi.org/10.1038/npp.2015.231.
21. Walker CK, Anderson KW, Milano KM, et al. Trophoblast inclusions are significantly increased in the Placentas of children in families at risk for Autism. Biol Psychiat. 2013;74(3):204–11. https://doi.org/10.1016/j.biopsych.2013.03.006.
22. Sedlmayr P, Blaschitz A, Stocker R. The role of placental tryptophan catabolism. Front Immunol. 2014;5. https://doi.org/10.3389/fimmu.2014.00230.
23. Walsh JJ, Christoffel DJ, Heifets BD, et al. 5-HT release in Nucleus Accumbens rescues Social deficits in Mouse Autism Model. Nature. 2018;560(7720):589–94. https://doi.org/10.1038/s41586-018-0416-4.
24. Goeden N, Velasquez J, Arnold KA, et al. Maternal inflammation disrupts fetal Neurodevelopment Via increased placental output of serotonin to the fetal brain. J Neurosci. 2016;36(22):6041–9. https://doi.org/10.1523/JNEUROSCI.2534-15.2016.
25. Muller CL, Anacker AM, Rogers TD, et al. Impact of maternal serotonin transporter genotype on placental serotonin, fetal forebrain serotonin, and neurodevelopment. Neuropsychopharmacol. 2017;42(2):427–36. https://doi.org/10.1038/npp.2016.166.
26. Patrick RP, Ames BN. Vitamin D hormone regulates serotonin synthesis. Part 1: relevance for Autism. Faseb J. 2014;28(6):2398–413. https://doi.org/10.1096/fj.13-246546.
27. Xiao L, Yan J, Yang T, et al. Fecal microbiome transplantation from children with Autism Spectrum Disorder modulates Tryptophan and Serotonergic Synapse Metabolism and induces altered behaviors in germ-free mice. Msystems. 2021;6(2). https://doi.org/10.1128/mSystems.01343-20.
28. Liu Y, Shan L, Liu T, et al. Molecular and Cellular mechanisms of the First Social Relationship: a conserved role of 5-HT from mice to monkeys, Upstream of Oxytocin. Neuron. 2023. https://doi.org/10.1016/j.neuron.2023.02.010.
29. Choi W, Namkung J, Hwang I, et al. Serotonin signals through a gut-liver Axis to regulate hepatic steatosis. Nat Commun. 2018;9(1). https://doi.org/10.1038/s41467-018-07287-7.
30. Karahoda R, Horackova H, Kastner P, et al. Serotonin Homeostasis in the Materno-Foetal interface at term: role of transporters (SERT/SLC6a4 and OCT3/SLC22a3) and Monoamine Oxidase a (MAO-a) in Uptake and Degradation of Serotonin by Human and Rat Term Placenta. Acta Physiol. 2020;229(4). https://doi.org/10.1111/apha.13478.
31. Gandal MJ, Edgar JC, Ehrlichman RS, Mehta M, Roberts TPL, Siegel SJ. Validating Γ oscillations and delayed auditory responses as translational biomarkers of Autism. Biol Psychiat. 2010;68(12):1100–6. https://doi.org/10.1016/j.biopsych.2010.09.031.
32. Roullet FI, Lai JK, Foster JA. In Utero exposure to Valproic Acid and Autism–A Current Review of Clinical and Animal studies. Neurotoxicol Teratol. 2013;36:47–56. https://doi.org/10.1016/j.ntt.2013.01.004.
33. Malassine A, Frendo JL, Evain-Brion D. A comparison of placental development and endocrine functions between the Human and Mouse Model. Hum Reprod Update. 2003;9(6):531–9. https://doi.org/10.1093/humupd/dmg043.
34. Zhao Q, Dai W, Chen HY et al. Prenatal Disruption of Blood–Brain Barrier Formation Via Cyclooxygenase Activation Leads to Lifelong Brain Inflammation. Proceedings of the National Academy of Sciences. 2022;119(15). https://doi.org/10.1073/pnas.2113310119
35. Ahn C, Yang H, Lee D, An B, Jeung E. Placental claudin expression and its regulation by endogenous sex steroid hormones. Steroids. 2015;100:44–51. https://doi.org/10.1016/j.steroids.2015.05.001.
36. Osman HC, Moreno R, Rose D, Rowland ME, Ciernia AV, Ashwood P. Impact of maternal Immune activation and sex on placental and fetal brain cytokine and gene expression profiles in a Preclinical Model of Neurodevelopmental disorders. J Neuroinflamm. 2024;21(1):118. https://doi.org/10.1186/s12974-024-03106-7.
37. Meyer U. Prenatal poly(I:C) exposure and other Developmental Immune Activation models in Rodent systems. Biol Psychiat. 2014;75(4):307–15. https://doi.org/10.1016/j.biopsych.2013.07.011.
38. Liang Z, Wang Q, Liao H, et al. Artificially Engineered Antiferromagnetic Nanoprobes for ultra-sensitive histopathological level magnetic resonance imaging. Nat Commun. 2021;12(1). https://doi.org/10.1038/s41467-021-24055-2.
39. Salphati L, Heffron TP, Alicke B, et al. Targeting the PI3K pathway in the brain–efficacy of a PI3K inhibitor optimized to Cross the blood-brain barrier. Clin Cancer Res. 2012;18(22):6239–48. https://doi.org/10.1158/1078-0432.CCR-12-0720.
40. Leach L, Lammiman MJ, Babawale MO, et al. Molecular Organization of tight and Adherens junctions in the human placental vascular tree. Placenta. 2000;21(5–6):547–57. https://doi.org/10.1053/plac.2000.0541.
41. Kobayashi K, Miwa H, Yasui M. Progesterone maintains amniotic tight junctions during Midpregnancy in mice. Mol Cell Endocrinol. 2011;337(1–2):36–42. https://doi.org/10.1016/j.mce.2011.01.019.
42. Kobayashi K, Inai T, Shibata Y, Yasui M. Dynamic changes in amniotic tight junctions during pregnancy. Placenta. 2009;30(10):840–7. https://doi.org/10.1016/j.placenta.2009.07.009.
43. Vento-Tormo R, Efremova M, Botting RA, et al. Single-cell Reconstruction of the early maternal–fetal interface in humans. Nature. 2018;563(7731):347–53. https://doi.org/10.1038/s41586-018-0698-6.
44. Efremova M, Vento-Tormo M, Teichmann SA, Vento-Tormo R, CellPhoneDB. Inferring cell–cell communication from combined expression of Multi-subunit ligand–receptor complexes. Nat Protoc. 2020;15(4):1484–506. https://doi.org/10.1038/s41596-020-0292-x.
45. Arenas-Hernandez M, Sanchez-Rodriguez EN, Mial TN, Robertson SA, Gomez-Lopez N. Isolation of Leukocytes from the murine tissues at the maternal-fetal interface. J Visualized Experiments. 2015;99e52866. https://doi.org/10.3791/52866.
46. Wang K, Zhou W, Jin X, et al. Enhanced brain delivery of Hypoxia-Sensitive liposomes by Hydroxyurea for Rescue Therapy of Hyperacute ischemic stroke. Nanoscale. 2023;15(27):11625–46. https://doi.org/10.1039/D3NR01071F.
47. Wang K, Zhou W, Wen L, et al. The Protective effects of Axitinib on Blood-Brain Barrier Dysfunction and Ischemia-Reperfusion Injury in Acute ischemic stroke. Exp Neurol. 2024;379:114870. https://doi.org/10.1016/j.expneurol.2024.114870.
48. Yu T, Jin X, Yu F, et al. Tumor and dendritic cell dual-targeting Nanocarriers maximize the therapeutic potential of IDO1 inhibitor in vivo. Nano Res. 2022;15(10):9204–14. https://doi.org/10.1007/s12274-022-4597-7.
49. Ranzil S, Ellery S, Walker DW, et al. Disrupted placental serotonin synthetic pathway and increased placental serotonin: potential implications in the pathogenesis of human fetal growth restriction. Placenta. 2019;84:74–83. https://doi.org/10.1016/j.placenta.2019.05.012.
50. Ho ATV, Palla AR, Blake MR et al. Prostaglandin E2 is Essential for Efficacious Skeletal Muscle Stem-Cell Function, Augmenting Regeneration and Strength. Proceedings of the National Academy of Sciences. 2017:201705420. https://doi.org/10.1073/pnas.1705420114
51. So JY, Skrypek N, Yang HH, et al. Induction of DNMT3B by PGE2 and IL6 at distant metastatic sites promotes epigenetic modification and breast Cancer colonization. Cancer Res. 2020;80(12):2612–27. https://doi.org/10.1158/0008-5472.CAN-19-3339.
52. Johannessen LC, Burns ML, Baftiu A, et al. Pharmacokinetic variability of Valproate in Women of Childbearing Age. Epilepsia. 2017;58(10):e142–6. https://doi.org/10.1111/epi.13872.
53. Patsalos PN, Berry DJ, Bourgeois BFD, et al. Antiepileptic Drugsbest Practice guidelines for Therapeutic Drug Monitoring: A position paper by the Subcommission on Therapeutic Drug Monitoring, ILAE Commission on therapeutic strategies. Epilepsia. 2008;49(7):1239–76. https://doi.org/10.1111/j.1528-1167.2008.01561.x.
54. Mandel-Brehm C, Salogiannis J, Dhamne SC, Rotenberg A, Greenberg ME. Seizure-Like Activity in a Juvenile Angelman Syndrome Mouse Model

is Attenuated by Reducing Arc Expression. Proceedings of the National Academy of Sciences. 2015;112(16):5129-34. https://doi.org/10.1073/pnas.1504809112
55. Hsiao EY, McBride SW, Hsien S, et al. Microbiota modulate behavioral and Physiological Abnormalities Associated with Neurodevelopmental disorders. Cell. 2013;155(7):1451–63. https://doi.org/10.1016/j.cell.2013.11.024.
56. SILVERMAN JL, TOLU SS, BARMAN CL, CRAWLEY JN. Repetitive self-grooming behavior in the BTBR mouse model of Autism is blocked by the MGluR5 Antagonist MPEP. Neuropsychopharmacol (New York N Y). 2010;35(4):976–89. https://doi.org/10.1038/npp.2009.201.
57. Angoa-Pérez M, Kane MJ, Briggs DI, Francescutti DM, Kuhn DM. Marble Burying and Nestlet Shredding as tests of repetitive, compulsive-like behaviors in mice. J Visualized Experiments. 2013;8210.3791/50978.
58. Won H, Lee H, Gee HY, et al. Autistic-like Social Behaviour in Shank2-Mutant mice improved by restoring NMDA receptor function. Nature. 2012;486(7402):261–5. https://doi.org/10.1038/nature11208.
59. Foote M, Qiao H, Graham K, Wu Y, Zhou Y. Inhibition of 14-3-3 proteins leads to Schizophrenia-related behavioral phenotypes and synaptic defects in mice. Biol Psychiat. 2015;78(6):386–95. https://doi.org/10.1016/j.biopsych.2015.02.015.
60. Meireson A, Devos M, Brochez L. IDO expression in Cancer: different compartment. Different Functionality? Front Immunol. 2020;11. https://doi.org/10.3389/fimmu.2020.531491.
61. Mezrich JD, Fechner JH, Zhang X, Johnson BP, Burlingham WJ, Bradfield CA. An Interaction between Kynurenine and the Aryl Hydrocarbon Receptor Can Generate Regulatory T Cells. J Immunol. 2010;185(6):3190–8. https://doi.org/10.4049/jimmunol.0903670.
62. Nguyen NT, Kimura A, Nakahama T et al. Aryl Hydrocarbon Receptor Negatively Regulates Dendritic Cell Immunogenicity Via a Kynurenine-Dependent Mechanism. Proceedings of the National Academy of Sciences. 2010;107(46):19961-6. https://doi.org/10.1073/pnas.1014465107
63. Hennequart M, Pilotte L, Cane S, et al. Constitutive IDO1 expression in human tumors is driven by Cyclooxygenase-2 and mediates intrinsic Immune Resistance. Cancer Immunol Res. 2017;5(8):695–709. https://doi.org/10.1158/2326-6066.CIR-16-0400.
64. Obermajer N, Muthuswamy R, Lesnock J, Edwards RP, Kalinski P. Positive feedback between PGE2 and COX2 redirects the differentiation of human dendritic cells toward stable myeloid-derived suppressor cells. Blood. 2011;118(20):5498–505. https://doi.org/10.1182/blood-2011-07-365825.
65. Gaspar P, Cases O, Maroteaux L. The Developmental Role of Serotonin: News from Mouse Molecular Genetics. Nat Rev Neurosci. 2003;4(12):1002–12. https://doi.org/10.1038/nrn1256.
66. Côté F, Fligny C, Bayard E et al. Maternal Serotonin is Crucial for Murine Embryonic Development. Proceedings of the National Academy of Sciences - PNAS. 2007;104(1):329 – 34. https://doi.org/10.1073/pnas.0606722104
67. Vuong HE, Pronovost GN, Williams DW, et al. The maternal Microbiome modulates fetal neurodevelopment in mice. Nature. 2020;586(7828):281–6. https://doi.org/10.1038/s41586-020-2745-3.
68. Muller CL, Anacker AM, Rogers TD, et al. Impact of maternal serotonin transporter genotype on placental serotonin, fetal forebrain serotonin, and neurodevelopment. Volume 42. Neuropsychopharmacology; 2016. pp. 427–36. (New York, N.Y.). 210.1038/npp.2016.166.
69. Hoffmann D, Dvorakova T, Schramme F, Stroobant V, Van den Eynde BJ. Tryptophan 2,3-Dioxygenase expression identified in murine decidual stromal cells is not essential for feto-maternal tolerance. Front Immunol. 2020;11:601759. https://doi.org/10.3389/fimmu.2020.601759.
70. Iwahashi N, Yamamoto M, Nanjo S, Toujima S, Minami S, Ino K. Downregulation of Indoleamine 2, 3-Dioxygenase expression in the Villous Stromal endothelial cells of Placentas with Preeclampsia. J Reprod Immunol. 2017;119:54–60. https://doi.org/10.1016/j.jri.2017.01.003.
71. Zardoya-Laguardia P, Blaschitz A, Hirschmugl B, et al. Endothelial indoleamine 2,3-Dioxygenase-1 regulates the placental vascular tone and is deficient in Intrauterine Growth Restriction and Pre-eclampsia. Sci Rep-Uk. 2018;8(1). https://doi.org/10.1038/s41598-018-23896-0.
72. Wei H, Liu S, Lian R et al. Abnormal expression of Indoleamine 2, 3-Dioxygenase in human recurrent miscarriage. Reproductive sciences (Thousand Oaks, Calif.). 2020;27(8):1656–64. https://doi.org/10.1007/s43032-020-00196-5
73. Santillan MK, Pelham CJ, Ketsawatsomkron P, et al. Pregnant mice lacking indoleamine 2,3-Dioxygenase exhibit Preeclampsia Phenotypes. Physiol Rep. 2015;3(1):e12257. https://doi.org/10.14814/phy2.12257.
74. MUNN DH, ZHOU M, ATTWOOD JT, et al. Prevention of allogeneic fetal rejection by Tryptophan Catabolism. Sci (American Association Advancement Science). 1998;281(5380):1191–3.
75. Mellor AL, Sivakumar J, Chandler P, et al. Prevention of T Cell-Driven complement activation and inflammation by Tryptophan Catabolism during pregnancy. Nat Immunol. 2001;2(1):64–8. https://doi.org/10.1038/83183.
76. Nishizawa H, Hasegawa K, Suzuki M, et al. Mouse model for allogeneic Immune reaction against Fetus recapitulates human Pre-eclampsia. J Obstet Gynaecol re. 2007;184704915. https://doi.org/10.1111/j.1447-0756.2007.00679.x.
77. Prasanna G, Carreiro S, Anderson S, et al. Effect of PF-04217329 a Prodrug of a selective prostaglandin EP2 agonist on intraocular pressure in preclinical models of Glaucoma. Exp Eye Res. 2011;93(3):256–64. https://doi.org/10.1016/j.exer.2011.02.015.
78. Schachar RA, Raber S, Courtney R, Zhang MA, Phase. 2, Randomized, Dose-Response Trial of Taprenepag Isopropyl (PF-04217329) Versus Latanoprost 0.005% in Open-Angle Glaucoma and Ocular Hypertension. Curr Eye Res. 2011;36(9):809 – 17. https://doi.org/10.3109/02713683.2011.593725
79. Coleman RA, Woodrooffe AJ, Clark KL, et al. The Affinity, intrinsic activity and selectivity of a structurally novel EP(2) receptor agonist at Human Prostanoid receptors. Brit J Pharmacol. 2019;176(5):687–98. https://doi.org/10.1111/bph.14525.
80. Woodward DF, Jones RL, Narumiya S. International Union of Basic and Clinical Pharmacology. LXXXIII: classification of Prostanoid receptors, updating 15 years of Progress. Pharmacol Rev. 2011;63(3):471–538. https://doi.org/10.1124/pr.110.003517.
81. Fischer DP, Griffiths AL, Lui S, et al. Distribution and function of prostaglandin E2 receptors in mouse Uterus: Translational Value for Human Reproduction. J Pharmacol Exp Ther. 2020;373(3):381–90. https://doi.org/10.1124/jpet.119.263509.
82. Steinwall M, Akerlund M, Bossmar T, Nishii M, Wright M. ONO-8815Ly, an EP2 agonist that markedly inhibits uterine contractions in women. Bjog-Int J Obstet Gy. 2004;111(2):120–4. https://doi.org/10.1046/j.1471-0528.2003.00016.x.
83. Sitruk-Ware R, Spitz IM. Pharmacological properties of Mifepristone: Toxicology and Safety in Animal and Human studies. Contraception. 2003;68(6):409–20. https://doi.org/10.1016/S0010-7824(03)00171-9.
84. Zhu H, Jia X, Ren M, et al. Mifepristone Treatment in pregnant murine Model Induced Mammary Gland Dysplasia and Postpartum Hypogalactia. Front Cell Dev Biol. 2020;8:102. https://doi.org/10.3389/fcell.2020.00102.
85. He Q, Yang B, Wang W, Wu H, Fang R. Synergistic effects of DL111-IT in combination with Mifepristone and Misoprostol on termination of early pregnancy in Preclinical studies. Contraception. 2003;68(4):289–95. https://doi.org/10.1016/S0010-7824(03)00179-3.
86. Bianchi PKFD, Leandro RM, Poscai AN, Yoshinaga T, Gonçalez PO, Kfoury Junior JR. Progesterone decreases in Vitro Indoleamine 2, 3-Dioxygenase expression in dendritic and CD4 + cells from maternal-fetal interface of rats. Immunol Invest. 2017;46(5):447–59. https://doi.org/10.1080/08820139.2017.1296856.
87. Lajko A, Meggyes M, Polgar B, Szereday L. The immunological effect of Galectin-9/TIM-3 pathway after low dose Mifepristone Treatment in mice at 14.5 day of pregnancy. PLoS ONE. 2018;13(3):e0194870. https://doi.org/10.1371/journal.pone.0194870.
88. Bonnin A, Goeden N, Chen K, et al. A transient placental source of serotonin for the fetal forebrain. Nature. 2011;472(7343):347–50. https://doi.org/10.1038/nature09972.
89. Bonnin A, Levitt P. Fetal, maternal, and placental sources of serotonin and New implications for Developmental Programming of the brain. Neuroscience. 2011;197:1–7. https://doi.org/10.1016/j.neuroscience.2011.10.005.
90. Braun AE, Mitchel OR, Gonzalez TL, et al. Sex at the interface: the origin and impact of sex differences in the Developing Human Placenta. Biol Sex Differ. 2022;13(1):50. https://doi.org/10.1186/s13293-022-00459-7.
91. Gonzalez TL, Sun T, Koeppel AF, et al. Sex differences in the Late First Trimester Human Placenta Transcriptome. Biol Sex Differ. 2018;9(1):4. https://doi.org/10.1186/s13293-018-0165-y.
92. Braun AE, Muench KL, Robinson BG, Wang A, Palmer TD, Winn VD. Examining sex differences in the human placental transcriptome during the first fetal androgen peak. Reprod Sci. 2021;28(3):801–18. https://doi.org/10.1007/s43032-020-00355-8.

Publisher's note